Regional environmental drivers of Kemp's ridley sea turtle somatic growth variation

Matthew D. Ramirez[1]*, Larisa Avens[2], Lisa R. Goshe[2], Melissa L. Snover[3], Melissa Cook[4], Heather L. Haas[5], and Selina S. Heppell[1]

[1]Oregon State University, Department of Fisheries and Wildlife, Corvallis, Oregon, 97331, USA
[2]NOAA National Marine Fisheries Service, Southeast Fisheries Science Center, Beaufort Laboratory, North Carolina, 28516, USA
[3]Population Ecology Services, Pago Pago, 96799, American Samoa
[4]NOAA National Marine Fisheries Service, Southeast Fisheries Science Center, Pascagoula, Mississippi, 39567, USA
[5]NOAA National Marine Fisheries Service, Northeast Fisheries Science Center, Woods Hole, Massachusetts, 02543, USA

*E–mail: mdramirez@uri.edu
*Address: 215 South Ferry Road, Narragansett, RI 02889
*ORCID ID: https://orcid.org/0000-0002-9628-8517

Abstract

Many environmental processes influence animal somatic growth rates. However, elucidating specific drivers of somatic growth variation has been challenging for marine megafauna. Using a 20+ year dataset of somatic growth generated through skeletochronology, we evaluated the relationship between multiple region-wide environmental factors—the *Deepwater Horizon* (*DWH*) oil spill, increasing population density, climate variability—and age- and region-specific Kemp's ridley sea turtle (*Lepidochelys kempii*) somatic growth. We observed significant, multi-year reductions in mean oceanic (age 0) and small neritic (age 2–5) juvenile growth rates beginning in 2012 for turtles stranded along the U.S. Gulf of Mexico (GoM) and Atlantic Coasts, which resulted in a reduction in mean size-at-age. We hypothesize this growth decline is related to long-term deleterious effects of the *DWH* oil spill on benthic and oceanic food webs in the GoM. Additionally, regional climate indices were strongly correlated with oceanic juvenile growth with a 2-yr lag (cross-correlation = –0.57 to 0.60), whereas GoM small neritic juvenile growth was strongly related to population abundance metrics. Generalized additive models that included all examined environmental covariates indicated that the drivers of the 2012 growth rate decline had the strongest effect on Kemp's ridley growth rates between 1995 and 2015, but that additive or synergistic effects of both climate variability and changing population abundance are likely for certain life stages. Continued collection of sea turtle humeri is needed to further clarify mechanisms underpinning the observed growth patterns given the coincidental timing of changes in environmental parameters examined herein.

Keywords: somatic growth rates, *Lepidochelys kempii*, density-dependence, climate effects, skeletochronology, environmental covariates, Gulf of Mexico

Introduction

A suite of natural and anthropogenic stressors have reshaped marine ecosystems over the past century through cascading effects on animal populations and the habitats they occupy (Halpern et al. 2008; Rocha et al. 2014; McCauley et al. 2015). Numerous studies have characterized single stressor effects on marine species, but fewer have examined species response to cumulative or integrative effects of multiple environmental stressors, particularly in long-lived, higher order marine megafauna (Crain et al. 2008; Bjorndal et al. 2013). As the population dynamics of long-lived species are highly sensitive to small changes in demographic rates (Heppell et al. 2000), increasing insight into environmental effects on growth, survival, and reproduction may help improve understanding of population and community dynamics, and ultimately aid the development of conservation and management strategies for protected species. Moreover, disentangling the relative influence of myriad environmental stressors on animal populations and ecosystems is essential to predicting future ecosystem response to perturbation. Sea turtles provide an ideal system to investigate the influence of multiple environmental phenomena on demographic rates because most species retain annual records of somatic growth in their humerus bones, similar to growth rings in trees and otoliths in fish, that can be collected from dead stranded turtles (Avens & Snover 2013), and, as ectotherms, their growth rates are highly influenced by environmental conditions.

The critically endangered Kemp's ridley sea turtle (*Lepidochelys kempii*) is a particularly appealing model species to evaluate environmental drivers of somatic growth rates. First, humerus bones have been collected from dead stranded turtles since the early 1990s (Snover and Hohn 2004; Avens et al. 2017), providing a unqiue sample set for growth analysis. Second, their global distribution is largely restricted to the Gulf of Mexico (GoM) and U.S. Atlantic (Musick

and Limpus 1997), areas that are experiencing rapid environmental change including a climate-driven ecological regime shift in the 1990s (Sanchez-Rubio et al. 2011; Karnauskas et al. 2015) and the 2010 *Deepwater Horizon* (*DWH*) oil spill (DWH NRDA Trustees 2016). The current understanding of Kemp's ridley life history suggests juveniles that reside in benthic GoM and U.S. Atlantic Coast habitats are geographically isolated from one another, with some proportion of turtles entering the U.S. Atlantic Coast at age 1 or 2 following the GoM oceanic life stage and not returning to the GoM until maturity (Putman et al. 2013, Caillouet et al. 2016, Avens et al. *in review*). This geographic isolation of two components of the population provides a natural experiment to examine *DWH* oil spill effects on sea turtle growth rates and potentially separate them from other region-wide environmental stressors. Lastly, the Kemp's ridley population grew exponentially (12–16% per year) through the 1990s and 2000s following decades of successful conservation and management (NMFS and USFWS 2015). This, combined with a robust record of nest and hatchling production for nearly the entire species, provides the opportunity to evaluate density dependent effects on their somatic growth rates (Caillouet et al. 2016, 2018).

Environmental impacts of the *DWH* oil spill and impact mitigation efforts were unprecedented in their spatiotemporal and ecological scale (DWH NRDA Trustees 2016; Beyer et al. 2016; Berenshtein et al. 2020). Negative effects of the *DWH* oil spill on somatic growth rates have been documented in a wide range of fish and invertebrate species (e.g., Rozas et al. 2014; Brown-Peterson et al. 2016; Herdter et al. 2017; Perez et al. 2017), but impacts on marine megafauna demographic rates are less understood. However, long-term impacts remain a significant concern given the continued deterioration of the health of GoM bottlenose dolphins and the clear decadal impacts of the 1989 *Exxon Valdez* oil spill on marine ecosystems and animal demographic rates (Peterson et al. 2003; Kellar et al. 2017). Immediate effects on sea

92 turtle survival and physiology are well-documented, but otherwise much remains unknown about
93 their response to this anthropogenic disturbance (McDonald et al. 2017; Mitchelmore et al. 2017;
94 Stacy et al. 2017; Wallace et al. 2017). Sublethal or indirect effects of the *DWH* oil spill on sea
95 turtle health may be responsible for a general decline in nutritional condition of stranded sea
96 turtles since 2012 and a reduction in juvenile Kemp's ridley growth rates in Mississippi since
97 2010 (Stacy 2015; Coleman et al. 2016).

98 Following decades of conservation and management, the abundance of all Kemp's ridley
99 life stages grew rapidly between 1990 and 2009 (Heppell et al. 2004; NMFS and USFWS 2015).
100 Unexpectedly, annual nest counts have fluctuated widely since 2010 and one hypothesis is that
101 density dependent processes may be acting on the population (Gallaway et al. 2016; Caillouet et
102 al. 2016, 2018). While the current population is less than 10% of its estimated historic size
103 (Bevan et al. 2016), long-term alteration and degradation of GoM ecosystems, including
104 reductions in important food resources (e.g., blue crab *Callinectes sapidus*; VanderKooy 2013),
105 may have lowered the potential carrying capacity of the GoM for sea turtles and other marine top
106 predators (Heppell et al. 2007; Caillouet 2014). Most support for this hypothesis is derived from
107 analyses of the species' nesting trends (Gallaway et al. 2016; Caillouet et al. 2016, 2018;
108 Kocmoud et al. 2019), which are confounded after 2010 with unknown effects of the *DWH* oil
109 spill, and the observation of increasing breeding intervals for Kemp's ridleys nesting in Texas
110 from 2008 to 2016 (Shaver et al. 2016). However, other environmental factors, such as colder
111 temperatures on the foraging grounds during the winter of 2009–2010 (Lamont and Fujisaki
112 2014; Gallaway et al. 2016), may underpin this change in breeding interval and additional
113 investigations are needed to evaluate whether density dependent processes are influencing
114 Kemp's ridley demographic rates.

115 Climate variability is a primary driver of spatiotemporal variability in ocean productivity,
116 and abrupt changes in climate forcing often precipitate ecological regime shifts (Rocha et al.
117 2014). Within the North Atlantic Ocean, an ecological regime shift occurred in the late-1990s as
118 a result of an abrupt warming of the ocean that coincided with one of the strongest El Niño
119 events on record as well as a shift from the cool to warm phase of the Atlantic Multidecadal
120 Oscillation (Sanchez-Rubio et al. 2011; Luczak C. et al. 2011; Reid and Beaugrand 2012;
121 Beaugrand et al. 2013; Karnauskas et al. 2015). This late-1990s regime shift has been linked to
122 reduced blue crab productivity in the GoM (Sanchez-Rubio et al. 2011), an important food
123 source for sea turtles, as well as declining growth rates in loggerhead (*Caretta caretta*), green
124 (*Chelonia mydas*), and hawksbill (*Eretmochelys imbricata*) sea turtles (Bjorndal et al. 2013,
125 2016, 2017). Similar declines in growth were observed in large juvenile and adult Kemp's
126 ridleys in the GoM from 1988 to 2009 and small juveniles from 2004 to 2009 (Avens et al.
127 2017), although links to climate variability have yet to be evaluated.
128 Here we examined temporal trends in juvenile Kemp's ridley sea turtle somatic growth
129 rates using a 20+ year dataset generated through skeletochronology. The primary objective of
130 this study was to quantify the relative influence of multiple regional environmental stressors—
131 the *DWH* oil spill, increasing population density, climate variability—on sea turtle growth rates.
132 We developed and tested a suite of hypotheses related to the differential effect of these factors
133 that are outlined here and in Figure 1. Given significant degradation of offshore and nearshore
134 habitats in the GoM following the 2010 *DWH* oil spill and the observed decline in GoM-stranded
135 turtle nutritional condition after 2012 (Stacy 2015; Beyer et al. 2016), we predicted that Kemp's
136 ridley growth rates would decline following the *DWH* oil spill for both oceanic and neritic
137 juveniles. We specifically predicted that this change would occur beginning in 2010 because

annual Kemp's ridley skeletal growth begins in spring, coincident with the timing of the *DWH* oil spill. Importantly, we predicted Atlantic turtle growth rates would not change after 2010 given their spatial isolation from the *DWH* oil spill. We predicted that density-dependent effects, if present, would result in declining growth rates beginning in the mid- to late-2000s, when population growth was the highest (NMFS and USFWS 2015). We expected density dependent effects would primarily manifest in small juvenile life stages in the GoM as they have the fastest growth rates and experience the greatest competition with conspecifics for resources due to their size and relative inexperience. We assumed Atlantic Kemp's ridley are not strongly influenced by intraspecific population density due to their relatively low abundance. Lastly, we predicted that climate effects would cause declining growth rates across all Kemp's ridley life stages and habitats beginning in the late-1990s in response to a regional regime shift as observed in other western North Atlantic sea turtle species (Bjorndal et al. 2016, 2017).

Materials and Methods

Sample collection and processing

Front flippers were collected from Kemp's ridleys that stranded on U.S. beaches by participants of the Sea Turtle Stranding and Salvage Network (Texas to Massachusetts, 1991 to 2017). Samples were obtained from turtles that either stranded dead or stranded alive but were later euthanized. Stranding location, date, and carapace length were recorded at the time of stranding (see Tables 1 and S1 for summary). Carapace length was measured as straightline (SCL) or curved (CCL) carapace length, notch to tip. In cases where only CCL was recorded, CCL was converted to SCL as described by Avens et al. (2017). This study utilizes and extends the growth datasets presented in Avens et al. (2017) (n = 333 turtles, GoM) and Snover et al.

(2007) (*n* = 144, Atlantic) to include growth histories obtained from a total of 784 turtles stranded along the U.S. GoM Coast and 451 turtles stranded along the U.S. Atlantic Coast. We assume that data derived from these strandings are generally reflective of turtles within each region but acknowledge that strandings represent a non-random sampling of the population. The likelihood of a dead turtle stranding is determined by its decomposition rate and drift time and distance which are in turn influenced by ocean current and temperature, factors that vary across space and time. And, the probability of a stranded turtle being observed is infleunced by coastline accessibility. Combined, we can assume strandings are biased towards turtles that die nearshore, perhaps skewing the dataset towards younger/smaller life stages that inhabit more shallow marine habitats, and exclude most oceanic stage turtles, though data for this life stage can be retained in the bones of small neritic juveniles.

Humerus bones were prepared and histologically processed as described by Avens and Snover (2013) and Avens et al. (2017). Tissue was removed from the humerus bones, which were then boiled and air dried for at least two weeks. A low speed isomet saw (Buehler) was used to cut a 2 to 3 mm thick cross-section from each bone just distal to the deltopectoral muscle insertion scar. Bone sections were fixed and decalcified using Cal Ex II (Fisher Scientific) or 10% neutral buffered formalin followed by RDO (Apex Engineering Corporation) and thin sectioned to 25 microns using a freezing-stage microtome (Leica) or cryostat (Thermo Scientific Microm HM 550). Thin sections were stained using diluted Ehrlich's hematoxylin, mounted onto microscope slides in 100% glycerin, and imaged using a digital camera fitted to a compound microscope. Growth mark analyses were performed using image analysis software (Olympus Microsuite and cellSens) and Adobe Photoshop (Adobe Systems). Two or three readers (of L. Avens, L. R. Goshe, M. Ramirez, M. Snover) independently analyzed the digital bone images to

184 determine the number and placement of lines of arrested growth (LAGs), which delimit the outer
185 edges of each skeletal growth mark (Snover and Hohn 2004), followed by a joint assessment to
186 reach consensus. Once consensus was reached, total humerus section diameter and the diameter
187 of each LAG were measured.
188
189 *Age and growth rate estimation*
190 Previous analyses validated annual LAG deposition in Kemp's ridley humerus bones
191 (Snover and Hohn 2004; Avens et al. 2017), allowing for characterization of age at stranding
192 through skeletochronology. Kemp's ridleys deposit a unique first-year growth mark, or
193 "annulus," that differs from subsequent marks (Snover and Hohn 2004). For bones where the
194 annulus was visible, an initial age estimate was determined directly from LAG counts. However,
195 bone resorption results in the loss of internal LAGs as sea turtles age (Zug et al. 1986),
196 preventing the direct assessment of turtle age in larger individuals where the annulus has been
197 resorbed. Therefore, for turtles where the annulus was not visible, a correction factor was
198 developed based on the relationship between LAG numbers and diameters from known age
199 individuals to estimate the number of LAGs lost to resorption for each bone (Parham and Zug
200 1997). An initial age estimate was then generated by adding the estimated number of resorbed
201 LAGs to the number of visible LAGs. A final age estimate at stranding was made by adjusting
202 initial age estimates to the nearest 0.25 years based on the mean hatch date for the population
203 (June) and individual stranding date. Given that LAG deposition occurs in late winter/early
204 spring and peak hatching for this species occurs during the summer (Snover & Hohn 2004), the
205 first-year growth mark denotes an age of ~0.75 years, the next LAG an age of 1.75 years, and so
206 on. Final age estimates were used to back-assign age estimates to individual LAGs. Similarly, a

207 calendar year was back assigned to each LAG based on the date of stranding.

208 There is a strong allometric relationship between humerus section diameter (HSD) and
209 SCL for Kemp's ridleys that allows for the back-calculation of body size estimates for
210 measurable LAGs (Snover and Hohn 2004; Avens et al. 2017). We characterized the HSD:SCL
211 relationship for newly processed turtle bones and combined that with the body proportional
212 hypothesis back-calculation technique (BPH; Francis 1990) to estimate SCL for every
213 measurable LAG, adjusted for turtle-specific SCL and HSD at death. Annual somatic growth
214 rates were then calculated by taking the difference between SCL estimates of successive LAGs.
215 In this way, multiple growth rate estimates were generated from each humerus bone (median = 3
216 per turtle, range = 1–8). Growth rate estimates were assigned to the calendar year associated with
217 the LAG that begins each growth interval.

218

219 *Environmental covariates*

220 To investigate environmental drivers of sea turtle somatic growth variation, we evaluated
221 the relative influence of the *DWH* oil spill, changing population density, and climate variability
222 on Kemp's ridley somatic growth rates. While these stressors are not encompassing of all major
223 environmental phenomena that may affect sea turtle growth rates, they were chosen for this
224 analysis because their potential influence matches the geographic scale encompassed by the
225 somatic growth rate dataset.

226 The relationship between growth and population density was investigated using two
227 population abundance metrics: (1) annual age class-specific abundance estimates obtained from
228 the most recent Kemp's ridley population model used for status assessment (i.e., model-
229 dependent metric; NMFS and USFWS 2015), and (2) cumulative annual hatchling production

230 from the species' index nesting beach in Tamaulipas, Mexico, which comprises over 85% of
231 nesting activity by the species (i.e., model-independent metric; data sourced from NMFS &
232 USFWS 2015). This species is unique among sea turtles in that nearly its entire annual
233 reproductive output is concentrated on only a handful of beaches in Mexico and South Texas that
234 have been monitored and protected continuously since 1978. This has allowed for the near-
235 complete census of nests laid and hatchlings produced from these beaches annually (NMFS and
236 USFWS 2015). The population model used to derive age-specific abundance estimates is a
237 deterministic age-based simulation model that uses known hatchling production since 1966 to
238 predict the number of nests laid annually (NMFS and USFWS 2015). Model-derived abundance
239 estimates by age-class are only used through 2009 given uncertainties in the cause of post-2009
240 nest countfluctuations—mortality likely increased due to the *DWH* oil spill (Wallace et al. 2017),
241 but other causes have also been proposed (Caillouet 2014; Caillouet et al. 2018; Kocmoud et al.
242 2019), creating substantial uncertainty in the underlying demographic processes for this species
243 after 2009. Trends in population abundance metrics are summarized in Figure S1.
244 To elucidate potential relationships between changes in broad scale climate patterns and
245 Kemp's ridley somatic growth variation, we considered three well-known modes of variability
246 [North Atlantic Oscillation (NAO), Atlantic Multidecadal Oscillation (AMO), and the El Niño
247 Southern Oscillation (ENSO)] that exert strong biophysical control on western North Atlantic
248 Ocean ecosystems (Giannini et al. 2001; Greene et al. 2013; Karnauskas et al. 2015).
249 Collectively, they influence ocean temperature, salinity, mixing, and circulation patterns that
250 affect the productivity, distribution, growth, and survival of animals across all trophic levels
251 (Drinkwater et al. 2003; Edwards et al. 2013; Karnauskas et al. 2015). For the NAO, we used the
252 winter (December to March) NAO index (wNAO) given that the NAO is thought to exert the

greatest influence on ocean ecosystems in the boreal winter (Drinkwater et al. 2003). For the ENSO, we used the Multivariate El Niño Southern Oscillation Index (MEI) Version 2, which integrates five meteorological variables: SST, surface air temperature, sea-level pressure, surface zonal winds, surface meridional winds, and Outgoing Longwave Radiation. Monthly AMO and bimonthly MEI data were obtained from NOAA's Earth System Research Laboratory (http://www.esrl.noaa.gov/psd/data/climateindices/) whereas wNAO data were obtained from the National Center for Atmospheric Research (https://climatedataguide.ucar.edu/climate–data/). Following Bjorndal et al. (2016, 2017), monthly AMO and bimonthly MEI data were averaged within a calendar year to create an annualized index used in all analyses.

Data Analysis

We employed a suite of statistical tools to evaluate the independent and synergistic effects of the *Deepwater Horizon* oil spill, population density, and climate variability on Kemp's ridley growth rates. Given the retrospective nature of this study, the statistical approach taken was necessarily correlative and we therefore do not conclusively attribute causation. In most cases, analyses were restricted to juvenile growth data—binned by age class (age 0, 1, 2–5, 6–9) to increase statistical power—given that adult turtle growth rate data are poorly represented in the dataset. These age classes align with known ontogenetic differences in somatic growth rates and are similar to those used in age-structured population models (Snover et al. 2007; NMFS and USFWS 2015). Age 0 (ages 0 to 0.75) and 1 (ages 0.75 to 1.75) align with the oceanic life stage but are separated here because growth rates differ between these ages and a fraction of Kemp's ridleys begin to recruit to neritic habitats at age 1 (Avens et al. *in review*). All other age classes represent neritic life stages, i.e., small neritic juveniles (ages 2–5), large neritic juveniles (age 6–

9). As somatic growth rates differ between Kemp's ridleys that inhabit the U.S. Gulf of Mexico and Atlantic Coast (Avens et al. 2017; Avens et al. *in review*; this study), growth data were analyzed separately for turtles that stranded on beaches in these regions for all age classes but age 0—all age 0 turtles are assumed to occupy the same oceanic habitats in the central GoM .

To investigate *DWH* oil spill effects on somatic growth rates we used two primary approaches: growth curve fits and temporal analysis. First, to examine population-level growth response, a family of von Bertalanffy growth functions (VBGFs) were fit to stranding size-at-age data for all turtles stranded before (1993–2009) and after (2011–2016) the *DWH* oil spill using non-linear least-squares regression. Eight models were considered to compare von Bertalanffy growth parameters (L_∞, asymptotic average length; K, Brody growth rate coefficient ; t_0, age when the average length is zero) between both time periods that ranged from including identical parameter estimates for each time period (1 L_∞, 1 K, 1 t_0) to including fully unique parameter estimates for each time period (2 L_∞, 2 K, 2 t_0), and all model subsets in between (Table 2). Akaike information criterion (AIC) and Akaike weights (w_i) were used to evaluate and compare models (Burnham and Anderson 2002). In addition, given the non-independence of the full growth dataset, VBGFs were fit to measured SCL and estimated age at stranding only, eliminating SCL and age data estimated from growth marks. VBGFs were fit using data from GoM-stranded turtles only; large juvenile and adult Kemp's ridleys are rare along the U.S. Atlantic Coast and are thus underrepresented in our dataset, preventing the generation of robust Atlantic Kemp's ridley VBGFs. Growth functions were implemented using the *FSA* (Ogle et al. 2018) and *nlstools* (Baty et al. 2015) packages in R (version 3.5.3; R Core Team 2019).

We implemented two complementary techniques, regression coding schemes and cutpoint structural analyses, to quantitatively examine temporal changes in somatic growth rates.

First, we used Reverse Helmert regression coding schemes to specifically compare growth rates in the years before (1995–2009) and after (2010–2015) the *DWH* oil spill. The advantage of this approach is that it allows for analysis of the entire growth dataset. We implemented coding schemes using age class-specific linear mixed-effects models that included annual growth rate as the dependent variable, year as the independent variable, and first-order autoregressive [AR(1)] covariance structure for growth increments within turtles. Turtle-specific random effects were also included to account for non-independence in the growth dataset—each turtle contributes multiple growth rates. We then used maximally selected rank statistics to identify the optimal cutpoint within each growth time series. This non-parametric approach was performed using the mean growth rates for each age class, is robust to small sample sizes (Hothorn and Lausen 2003; Müller and Hothorn 2004), and was implemented using the *coin* package in R (Zeileis et al. 2002; Hothorn et al. 2006).

Generalized Additive Models (GAMs) were used to examine relationships between population density metrics and mean age class-specific growth rates. Models included age-specific abundance (*Abund*) or cumulative hatchling production (*HatchProd*) as a fixed effect, an identity link, and a quasi-likelihood error function. Within each model, mean growth rates were weighted by sample size (i.e., number of growth rate estimates per year). For the oceanic life stages (age 0, age 1), age-specific growth rates were compared to the model-derived cumulative number of 0– and 1–year old turtles predicted to exist in a given year (metric 1) or the cumulative number of hatchlings produced in a given year and the year prior (t_0–t_{-1}) (metric 2). For the neritic life stages (age 2–5, age 6–9), age-specific growth rates were compared to the model–derived cumulative number of juvenile turtles (ages 2–5) predicted to exist in a given

year (metric 1) or the cumulative number of hatchlings produced two to five years in the past (t_{-2}–t_{-5}) (metric 2). Models were implemented in R using the *mgcv* package (Wood 2006).

We used cross-correlation to examine relationships between mean age class-specific growth rates and climate indices. Following Bjorndal et al. (2016), GAMs with AR(1) covariance structure were fit to the annualized climate data to reveal underlying trends since 1950 for the wNAO and AMO and since 1979 for the MEI. Mean age class-specific growth rates were then compared to lagged (0- to 5-yrs) smoothing spline fits generated from the GAMs using the *ccf* function in R (version 3.5.3; R Core Team 2019). Cross-correlation coefficients were used to measure the degree of similarity between the two time series.

Lastly, to directly compare the independent and synergistic effects of these environmental stressors on sea turtle growth rates, we performed an integrative analysis that incorporated the results of the aforementioned independent analyses into a family of GAMs for each age class. Models included various combinations of the three factors investigated as fixed effects, an identity link, and a quasi-likelihood error function. We weighted mean growth rates by sample size and used AIC and w_i to evaluate and compare models (Burnham and Anderson 2002).

Results

Age and Growth

SCL and age at stranding ranged from 4.2 to 69.1 cm SCL and 0 to 30.25 years for turtles stranded on U.S. GoM beaches. Turtles stranded on U.S. Atlantic Coast beaches were 19.3 to 66.7 cm SCL and 1.00 to 18.75 years old (Tables 1, S1). Although their contribution to the breeding population is not well understood (NMFS and USFWS 2015), documentation of tagged Atlantic turtles nesting on the species' primary nesting beach in Mexico suggests that Atlantic

Kemp's ridleys ultimately return to the GoM as large juveniles or maturing adults (Caillouet et al. 2015), resulting in relatively few adult animals on the Atlantic Coast. In total, skeletochronological analyses yielded 3647 annual growth rate estimates from 1235 turtles for the years 1988 to 2015 (Fig. 2). This constitutes the largest and most comprehensive dataset of Kemp's ridley somatic growth rates to date. Annual growth rates span ages 0 (first year of life) to 28.75 but data from younger ages (< 6 yrs) dominate the dataset (~75%) because younger/smaller turtles are the most abundant Kemp's ridley age classes in the population and thus constitute the majority of stranded turtles (Gallaway et al. 2016).

For both the GoM and Atlantic Coast, there were distinct spatiotemporal changes in humerus bone collection (Fig. 2). Prior to 2010, GoM samples were primarily obtained from turtles stranded in Texas and Florida, whereas after 2010 sample collection shifted to turtles stranded in Louisiana, Mississippi, and Alabama as part of the *DWH* oil spill response efforts. Along the U.S. Atlantic Coast, there was a similar shift in sample collection in 2014 and 2015 from turtles that stranded primarily in North Carolina and Virginia to turtles that stranded in Massachusetts. Using a general linear mixed model that accounted for year, age, AR(1) autocorrelation, and turtle-specific random effects, we found somatic growth rates did not differ within regions (Tukey's post hoc test, $p > 0.05$) but were significantly lower in turtles from the Atlantic Coast (Tukey's post hoc test, $p < 0.05$). Examination of age class-specific growth rates indicates that these regional differences in growth manifest as early as Age 1 and extend through the small neritic juvenile life stage (age 2–5) (Fig. 3). Regional differences in Kemp's ridley growth, size-at-age relationships, and maturation trajectories are further examined by Avens et al. (*in review*), whose analysis uses the same growth rate dataset presented herein.

366 The quantity of age class-specific somatic growth rate data was sparse for years
367 preceding 1995, so all temporal growth analyses begin in 1995 and generally extend through
368 2014 or 2015 (Fig. 3). The datasets for age 0, age 2–5$_{GoM}$, age 2–5$_{Atlantic}$, and age 6–9$_{GoM}$ turtles
369 are the largest and most continuous—all years have at least seven independent growth rate
370 estimates (Fig. 3). In contrast, significant data gaps exist for age 1$_{GoM}$, age 1$_{Atlantic}$, and age 6–
371 9$_{Atlantic}$ turtles and the datasets for age 6–9$_{GoM}$ and age 6–9$_{Atlantic}$ turtles only extend to 2012 and
372 2010, respectively. We thus urge caution when interpreting results from the age 1 and age 6–9
373 datasets given that they are discontinuous and do not reflect similar time frames as the data for
374 ages 0 and 2–5.
375
376 *Deepwater Horizon oil spill effects*
377 The von Bertalanffy growth models fit to GoM turtle stranding length-at-age data
378 suggested that somatic growth differed before and after the *DWH* oil spill (Table 2, Fig. 4). The
379 model with the lowest AIC score and highest individual Akaike weight (w_i of 0.305) included
380 common L_∞ and t_0 parameters but different K parameters for the two time periods (1993–2009
381 vs. 2011–2016; Table 2). Parameter estimates for the best model were L_∞ = 65.04, t_0 = 1.52, K
382 (pre-*DWH*) = 0.192, and K (post-*DWH*) = 0.178. However, the next three best models had ΔAIC
383 scores less than 2.0 and w_i values between 0.113 and 0.298. While the parameters that differed or
384 agreed between the two time periods varied in these models (common L_∞, different K and t_0;
385 different L_∞, K, and t_0; common t_0, different L_∞ and K), all included two separate K parameters.
386 The summed weights of the models that included separate K parameters for the two time periods
387 was 0.890, indicating overall support for a growth rate reduction in the GoM after the *DWH* oil
388 spill. Although we found some evidence for differences in K parameters, there was significant

389 overlap in the distributions of the stranding length-at-age data before and after the *DWH* oil spill
390 (Fig. 4), which suggests this apparent difference may not be biologically meaningful or that there
391 was not a systemic change in somatic growth across all U.S. GoM Kemp's ridley size classes.
392 Insufficient length-at-age data for larger/older Atlantic Kemp's ridleys, which are thought to
393 migrate back to the GoM prior to maturity (Caillouet et al. 2015), impeded our ability to fit von
394 Bertalanffy growth models for these turtles (but see Avens et al. *in review*).
395 Reverse Helmert regression coding schemes applied to the full somatic growth dataset
396 identified significant decreases in Kemp's ridley growth rates between 2011 and 2012 (Table 3).
397 Relative to pre-*DWH*, growth rates in 2012 declined by 1–2 cm yr^{-1} within the age 0 and age 2–
398 5_{GoM} time series and greater than 3 cm yr^{-1} within the age $2–5_{Atlantic}$ time series. Notably, this
399 analysis revealed that growth rates in 2013 (age 0, age $2–5_{GoM}$) and 2014 (age $2–5_{GoM}$, age 2–
400 $5_{Atlantic}$) were also significantly lower than pre-*DWH* growth rates. Relative to pre-*DWH*, growth
401 rates from 2012 to 2015 were lower by 8.1 % for age 0 turtles, 22.7 % for age $2–5_{GoM}$ turtles, and
402 30.7% for age $2–5_{Atlantic}$. Similar results were obtained using complementary cutpoint analyses,
403 which identified significant decreases in mean annual somatic growth rates between 2011 and
404 2012 for turtles in the oceanic (age 0; max$T$ = 3.14, p = 0.005) and small neritic juvenile life
405 stages in both the U.S. GoM (age $2–5_{GoM}$; max$T$ = 2.98, p = 0.008) and Atlantic Coast (age 2–
406 $5_{Atlantic}$; max$T$ = 3.37, p = 0.004) (Table 3, Fig. 3). The cutpoint analysis did not identify any
407 statistically significant changes in somatic growth rates for the age 1 and age 6–9 time series ($p <$
408 0.05), though regression coding identified a significant increase in age $1_{Atlantic}$ growth rates and
409 decrease in age $6–9_{Atlantic}$ growth rates 2014.
410 Taken together, these analyses provide evidence for a sharp decline in Kemp's ridley
411 growth rates in the years following the *DWH* oil spill. However, the results of the temporal

412 analyses did not align with our original hypotheses that predicted either an acute (H_{1A}) or chronic
413 (H_{1B}) *DWH* oil spill impact on somatic growth rates beginning in 2010 for turtles in the GoM
414 only (Fig. 1). Interestingly, this decline is evident, and proportionally greater, in Atlantic
415 stranded turtles, which we predicted to exhibit no temporal changes in growth rates around the
416 time of the *DWH* oil spill due to their spatial isolation. However, even with a decrease in growth
417 rates, GoM small neritic juveniles (age 2–5) still grew faster than Atlantic conspecifics.
418
419 *Density-dependent effects*
420 We found little support for density dependent effects of cumulative turtle abundance and
421 hatchling production on mean age class-specific somatic growth rates (Table S2). For all but age
422 2–5_{GoM}, GAMs revealed no significant relationship between these population density metrics and
423 somatic growth ($p > 0.05$)—mean annual growth rates did not decline with increasing predicted
424 juvenile abundance nor was there the presence of a threshold above which growth rates declined.
425 The GAM response functions for both population abundance metrics and both GoM and Atlantic
426 stranded turtles were generally similar (Figs. S2–S4).
427 Cumulative hatchling production was a significant ($p = 0.018$) predictor of age 2–5_{GoM}
428 somatic growth whereas cumulative age 2–5 abundance was only a marginally significant ($p =$
429 0.051) predictor (Table S2, Fig. 5). Growth rates at the highest age 2–5_{GoM} population
430 abundances were lower on average than those at lowest predicted population abundance,
431 although 95% confidence intervals surrounding the annual means at the highest and lowest
432 abundances overlapped extensively. Nevertheless, the shapes of this relationship for age 2–5_{GoM}
433 did align with our hypothesis related to density-dependent effects (H_2) on somatic growth rates
434 (Fig. 1), which predicted a threshold above which growth rates begin to decline.

435

436 *Climate effects*

437 Mean annual growth rates tended to poorly correlate with the annualized climate indices
438 with 0- to 5-year lags (Table S3). Cross correlations for most life stages (age 1, age 2–5, age 6–
439 9) were generally negligible to weak (cross correlations ≤ |0.40|), although cross correlations for
440 age 6–9_{GoM} with 4- and 5-yr lags were –0.53 and –0.59 for wNAO and 0.52 and 0.60 for AMO.
441 In contrast, mean annual growth rates exhibited moderate to strong correlations with all climate
442 indices for the oceanic life stage (age 0; Fig. 6). The highest, consistent cross correlation values
443 for age 0 included a 2-year lag (wNAO = 0.59; AMO = –0.57; MEI = 0.60). Cross correlations
444 values ≥ |0.50| were also observed for the wNAO and AMO with 3- to 4-yr lags, and the MEI
445 with 0- to 1-yr lags. The consistency in age class-specific growth patterns through time (Fig. 3)
446 generally do not align with our predicted climate growth response (Fig. 1: H_3) of declining
447 growth rates beginning in the late 1990s. However, our results suggest climate variability may
448 affect hatchling and oceanic juvenile growth during the oceanic life stage.

449 For the wNAO, positive cross correlations indicate that growth rates are higher when
450 winter weather conditions in the western North Atlantic are warmer and wetter (Drinkwater et al.
451 2003) and during periods of high river discharge, enhanced blue crab productivity, and reduced
452 *Sargassum* abundance in the GoM (Sanchez-Rubio et al. 2011, 2018). Similar conditions along
453 with cooler ocean temperatures are present during negative AMO phases (Karnauskas et al.
454 2015), which aligns with our observation of negative correlations between AMO and growth
455 rates (i.e., positive wNAO and negative AMO are coupled). Positive correlations between the
456 MEI and growth indicates growth rates increase with increasing ocean temperatures (Giannini et
457 al. 2001). However, our observation of declining oceanic stage turtle growth during a period of

458 warming suggest that indirect negative effects of increasing ocean temperatures on sea turtle
459 foraging habitat or prey may be negatively impacting their growth rates (Bjorndal et al. 2017).
460
461 *Integrative effects*
462 Three sets of GAMs were implemented to determine which environmental factors—
463 either independently or synergistically—were most strongly related to age 0, age 2–5_{GoM}, and
464 age 2–$5_{Atlantic}$ growth. Comparative models were restricted to these age classes because they
465 showed evidence of significant temporal, density, and climate effects within independent
466 analyses. The three metrics evaluated in these models were (1) the temporal shift (*TS*) in growth
467 observed in 2012, included as a categorical variable (TS_{pre} = 1995–2011, TS_{post} = 2012–2015);
468 (2) cumulative hatchling production (*HatchProd*), included as a continuous variable; and, (3) the
469 annualized GAM trend for the AMO index with a 2-year lag, included as a continuous variable.
470 We generated models that included all combinations of these covariates as fixed effects, resulting
471 in the evaluation of six models for each age class (i.e., *TS* + *HatchProd* + *AMO, TS* +
472 *HatchProd, TS* + *AMO, TS, HatchProd, AMO*). The *HatchProd* and *AMO* covariates displayed a
473 moderate to high degree of collinearity with variance inflation factors of ~ 6 and correlation
474 coefficients between 0.83 and 0.92, indicating that the coefficients in the global model (*TS* +
475 *HatchProd* + *AMO*) may be poorly estimated and that the p-values may be questionable
476 (Dormann et al. 2013). We include the model herein for comparison but urge caution when
477 interpreting their results.
478 Within each age class, multiple models had ΔAIC scores less than two and were thus
479 considered strong potential predictors of mean age class-specific growth rates (Table 4). In all
480 cases these top models included *TS* alone or in combination with *HatchProd* and *AMO*.

481 However, in most cases *HatchProd* and *AMO* were not statistically significant predictor
482 variables (Table 5). The *HatchProd* and *AMO* only models explained the least variation in
483 somatic growth for all age classes.
484 For age 0, the top model included *TS* and *HatchProd* as fixed effects based on AIC score
485 and Akaike weight. However, the next three best models were within 2 AIC, which included *TS*
486 + *HatchProd*, *TS* only, or *TS* + *HatchProd* + *AMO* as fixed effects. The cumulative Akaike
487 weight for these top four models was 1.00. and *TS* was the only statistically significant predictor
488 of mean age 0 growth rates in these top four models (Table 5).
489 For age 2–5_{GoM}, the best model included all three covariates as fixed effects and had an
490 Akaike weight of 0.49. Notably, all three covariates were statistically significant predictors of
491 age 2–5_{GoM} somatic growth rates within this top model. A second model, *TS* + *HatchProd*, was
492 within 0.29 AIC of this best model. Only *TS* was a statistically significant predictor of mean age
493 2–5_{GoM} growth rates in this second model (Table 5), although *HatchProd* was marginally
494 significant ($p = 0.072$). The cumulative Akaike weight of these top two models was 0.92.
495 For age 2–$5_{Atlantic}$, the top model included *TS* only and had an Akaike weight of 0.45.
496 Two additional models had ΔAIC scores less than two (*TS* + *HatchProd* and *TS* + *AMO*),
497 providing for a cumulative Akaike weight of 0.86 for the top three models. As for the age 0
498 models, *TS* was the only statistically significant predictor of mean age 2–$5_{Atlantic}$ growth rates
499 within the top age 2–$5_{Atlantic}$ models (Table 5).
500
501 **Discussion**
502 Marine ecosystems are experiencing unprecedented change due to the combined effect of
503 suites of environmental factors. As population responses to ecosystem change are manifested

504 through changes in animal demographic rates, establishing mechanistic links between
505 environmental stressors and demographic variation is fundamental to understanding and
506 predicting species population dynamics. Through an analysis of 20+ years of somatic growth rate
507 data, we show that juvenile Kemp's ridley sea turtles experienced a significant, multi-year
508 reduction in somatic growth from 2012 to 2015 that spanned multiple life stages (oceanic and
509 small neritic juveniles) and habitats (GoM and U.S Atlantic). Specific mechanisms underpinning
510 this population-wide temporal shift in growth remain elusive, but likely include direct and
511 indirect negative effects of the *DWH* oil spill. Cumulatively, drivers of this 2012 change in
512 somatic growth constitute the single greatest contributor to somatic growth variation in recent
513 decades among the environmental factors investigated, though our integrative analysis indicated
514 that regional climate variability and changing population density have likely had synergistic
515 effects on oceanic (climate only) and small neritic (climate + population density) juvenile
516 somatic growth rates in the GoM. Our results contrast with other post-*DWH* oil spill studies that
517 observed immediate effects on growth rates in invertebrates and fish in 2010 but align with
518 observations of declining stranded turtle nutritional condition in the northern GoM beginning in
519 2012 (Stacy 2015), a phenomena of unknown origin but that would likely reduce growth rates.
520
521 *Growth and the Deepwater Horizon oil spill*
522 We hypothesize that the 2012 reductions in growth observed across the species' U.S.
523 range result partially from indirect negative effects of the *DWH* oil spill on sea turtle health
524 mediated by ecosystem changes. We initially predicted a direct *DWH*-associated growth
525 response would manifest in 2010 for GoM turtle life stages only given the coincidence of the oil
526 spill and annual initiation of sea turtle somatic growth, and the observation of immediate changes

in other species' demographic rates (e.g., Rozas et al. 2014; Brown-Peterson et al. 2016; Herdter et al. 2017; Perez et al. 2017). However, the lack of a growth response in 2010 suggests the *DWH* oil spill may not have had immediate, direct impacts on sea turtle growth rates. Still, indirect negative effects are likely given the scale of the oil spill and whose impact may have taken years to transcend food webs to influence sea turtle demographic rates.

Chronic exposure to *DWH*-associated environmental toxins may threaten the long-term health of marine megafauna in the GoM, including sea turtles. Following the 1989 *Exxon Valdez* oil spill, chronic exposure to weathered oil entrained in sediments delayed the recovery of a wide range of taxa for decades due to long-term effects on species demographic rates (Peterson et al. 2003). Similar effects appear to be compromising the long-term health, reproductive success, and survival of GoM bottlenose dolphins (Schwacke et al. 2014, 2017; Lane et al. 2015; Kellar et al. 2017). Much like other mobile marine predators, sea turtles were exposed to *DWH*-associated environmental toxins for years following the oil spill due to its spatial overlap with key oceanic and neritic foraging grounds that they continued to use (Shaver et al. 2013; Hart et al. 2014; Wallace et al. 2017; Berenshtein et al. 2020). The leaching and resuspension of oil-contaminated sediments represents a continued, long-term threat to coastal GoM food webs (Murawski et al. 2016; Rouhani et al. 2017; Romero et al. 2017). Additionally, both oceanic and neritic sea turtles directly ingested spilled oil and absorbed polycyclic aromatic hydrocarbons (PAHs) into their tissues (Ylitalo et al. 2017; Reich et al. 2017), which can cause adverse physiological effects in animals such as reduced growth (e.g., Meador et al. 2006; Albers 2006).

Interestingly, the observed 2012 decline in somatic growth aligns with a simultaneous deterioration of neritic stranded turtle nutritional condition and shift in sea turtle foraging behavior in the northern GoM. Necropsies of juvenile Kemp's ridleys (25–60 cm SCL, ~2–9 yrs)

550 stranded in the northern GoM between 2010 and 2014 revealed significant reductions in the size
551 of turtle fat stores beginning in 2012 (Stacy 2015). Coincident with this change was a greater
552 association of sea turtles with fishing piers in Mississippi where turtles regularly attempted to eat
553 fishing bait (Coleman et al. 2016), a behavior previously linked to reduced growth rates in
554 Kemp's ridleys (Rudloe and Rudloe 2005). The integration of these findings with those herein
555 suggest a fundamental shift in the functioning of northern GoM food webs prior to 2012 that
556 impacted turtle foraging, nutritional condition, and inevitably growth. Causal factors for changes
557 in nutritional condition and foraging behaviors have not been identified, but the spatiotemporal
558 proximity to the *DWH* oil spill is conspicuous. Alternatively, these changes may relate to the
559 collapse of the Mississippi blue crab fishery in 2011, which has been attributed to freshwater
560 inundation from the opening of the Bonnet Carré Spillway (GSMFC 2015), but may also be
561 connected to negative effects of the *DWH* oil spill (Alloy et al. 2015; Giltz and Taylor 2017).
562 Comparisons of the nutritional status and growth histories of dead stranded turtles may improve
563 our understanding of temporal variability in Kemp's ridley growth dynamics.
564 Negative impacts of the *DWH* oil spill on oceanic habitats were severe and were
565 predicted to also impact the growth rates of oceanic stage turtles beginning in 2010. However,
566 much like the GoM small neritic juvenile life stage, we did not observe a significant decline in
567 oceanic stage turtle growth rates in 2010 but in 2012. All Kemp's ridleys associate with floating
568 *Sargassum* in GoM oceanic habitats for the first 1 to 3 years of life before recruiting to neritic
569 habitats along either the GoM or U.S. Atlantic Coast (Turtle Expert Working Group 2000; Avens
570 et al. *in review*). Following the oil spill, *Sargassum* tended to accumulate oil, become hypoxic,
571 and sink (Powers et al. 2013). The loss or compromisation of this critical habitat would have
572 ultimately increased predation rates, reduced prey availability, and increased the energetic costs

573 of foraging during this life stage (Witherington 2002). Given the vulnerability of oceanic stage
574 turtles, the lack of a 2010 and 2011 growth response may indicate stronger initial *DWH* effects
575 on survival rather than growth (McDonald et al. 2017). Interestingly, *Sargassum* abundance was
576 anomalously high in 2011 and 2012 throughout the tropical North Atlantic, which should have
577 renewed these habitats and provided oceanic stage turtles with optimal conditions for growth and
578 survival (Witherington et al. 2012; Gower et al. 2013; Powers et al. 2013). That growth rates
579 instead declined in 2012 and 2013 suggests either lingering effects of the *DWH* oil spill on these
580 food webs or the influence of another environmental stressor (outlined below).
581 The observation of a strong, proportionally greater decline in Atlantic small neritic
582 juvenile growth in 2012 was unexpected given our initial assumption that their growth rates
583 would not change following the *DWH* oil spill. The specific causal factors for this decline remain
584 unknown but could be related to negative effects of the *DWH* oil spill on GoM *Sargassum*
585 habitats. It is well established that early nutrition can impact life-time growth through 'silver
586 spoon' effects (Larsson and Forslund 1991; Madsen and Shine 2000; McAdam and Boutin 2003;
587 Gaillard et al. 2003), and many of the Atlantic Kemp's ridleys that exhibited reduced growth in
588 2012–2015 would have occupied GoM *Sargassum* habitats in 2010. Therefore, it is plausible that
589 cumulative impacts of the *DWH* oil spill on oceanic turtle habitats and physiology compromised
590 their long-term turtle health and were carried with them into non-impacted marine habitats both
591 within and outside the GoM (Putman et al. 2015). We still do not understand why Atlantic
592 Kemp's ridleys grow more slowly than their GoM counterparts (reviewed in Avens et al. 2017,
593 *in review*), but the underlying cause could have interacted with carryover effects of the *DWH* oil
594 to amplify their cumulative growth response and cause the proportionally greater decline in

595 Atlantic Kemp's ridley growth rates. Improved understanding of drivers of Atlantic Kemp's
596 ridley growth variation will be key to disentangling potential effects of the *DWH* oil spill.
597
598 *Interactive effects of multiple environmental stressors*
599 Although the driver of the post-2012 shift in growth was identified as the greatest single
600 contributor to Kemp's ridley somatic growth variation over the past twenty years, we found
601 support for additive or synergistic effect of changing population density and climate variability
602 on GoM turtle growth rates. Indeed, our integrative analysis identified all three environmental
603 factors as significant predictors of GoM small neritic juvenile somatic growth. One hypothesis
604 for the recent fluctuations in Kemp's ridley nest counts after a period of exponential growth is
605 that the carrying capacity of the GoM has been reached for this species (Gallaway et al. 2016;
606 Caillouet et al. 2016, 2018). Empirical support for this hypothesis, however, has been lacking
607 due to insufficient data independent of the nesting trends, which are confounded after 2010 with
608 unknown effects of the *DWH* oil spill (but see Shaver et al. 2016). Within both independent and
609 integrative analyses we found strong support for a statistically significant relationship between
610 population density metrics and GoM small neritic juvenile growth. Specifically, we observed
611 lower, more variable growth rates at the highest population densities and a multi-year declining
612 growth trend that began in the mid-2000s, which generally aligns with our initial predictions and
613 observations in Avens et al. (2017). However, these findings are equivocal. Growth rates at the
614 highest population densities (2010–2015) overlap considerably with growth rates at the lowest
615 population densities (1995–1999) (Fig. 5). Therefore, more research is needed, especially
616 extensions of the skeletochronology dataset, before we can confidently assert Kemp's ridley
617 population density is influencing their somatic growth rates. Importantly, our findings contrast

618 with those that have suggested that density dependent processes have influenced this population
619 as early as the year 2000 (Caillouet et al. 2018; Caillouet 2019).
620 Climate variability may also influence both oceanic and small neritic juvenile Kemp's
621 ridley growth rates in the GoM, though our independent and integrative analyses provide
622 conflicting results. Recent studies have linked decades-long declines in sea turtle growth rates in
623 the Caribbean Basin to a late-1990s climate-driven ecological regime shift (Bjorndal et al. 2013,
624 2016, 2017). Herein, cross-correlations between lagged climate indices and somatic growth rates
625 identified moderate to strong correlations for oceanic stage turtles but climate was not a
626 significant predictor within the integrative analysis. The opposite pattern was observed for GoM
627 small neritic juveniles, where the climate indices were poorly correlated with somatic growth
628 within the independent analysis but identified as a significant predictor in the top integrative
629 model. Conflicting results for small neritic juveniles may be due in part to issues with
630 collinearity between population density and climate metrics in the top integrative model which
631 could inflate variance in model parameters for one or both variables (Dormann et al. 2012).
632 These issues aside, as ectotherms, sea turtle growth rates would generally be expected to
633 correlate with temperature-driven climate indices such as the AMO and MEI, particularly during
634 the oceanic stage when they occupy epipelagic habitats and have limited capacity to fight ocean
635 currents. Therefore, changes in growth rates for oceanic stage turtles may reflect the synergistic
636 effects of regional climate variability on oceanic habitats and lingering impacts of the *DWH* oil
637 spill, whereas changes in growth rates for GoM small benthic juveniles may have been more
638 strongly influenced by interactive effects of the *DWH* oil spill and population density.
639 Our analysis focused on three environmental stressors with wide-reaching influence, but
640 many other environmental factors likely contributed to Kemp's somatic variation during the

641 study period, particularly for Atlantic turtles. Anomalous heatwaves occurred in the western
642 North Atlantic in 2012 and 2016 that caused widespread ecosystem change, including shifts in
643 species distributions and recruitment (Mills et al. 2013; Pershing et al. 2015, 2018; Henderson et
644 al. 2017). Though effects of these heatwaves on sea turtles remain unknown, negative effects of
645 rising temperatures on Kemp's ridley foraging habitats and prey could have indirectly impacted
646 their growth rates, a mechanism suggested to explain the declining growth trends in western
647 North Atlantic loggerhead, green, and hawksbill sea turtles in recent decades (Bjorndal et al.
648 2016, 2017). More broadly, local water temperatures hold the potential to substantially
649 contribute to somatic growth variation in this species given that its geographic distribution spans
650 greater than 20 degrees latitude (18°N to 43°N), thus a wide temperature range, and that parts of
651 the U.S. Atlantic Coast are warming faster than anywhere else in the world (Pershing et al.
652 2015). Establishing mechanistic links between sea turtle growth rates and local water
653 temperatures, such as through comparison of terminal humerus bone growth rates with local
654 temperature records, will be critical to understanding how sea turtles may respond to climate
655 change (Stubbs et al. 2020). A suite of other environmental factors—regional diet variation, prey
656 availability and distribution, intra-and inter-specific competition, genetics, migration distance
657 (see Avens et al. 2017, *in review;* Ramirez et al. 2020)—have also been identified as possible
658 contributors to Kemp's ridley somatic growth variation and warrant further study.
659
660 *Implications of reduced somatic growth rates*
661 Whether the observed growth declines represent a biologically meaningful change
662 requires further evaluation. Somatic growth and body size influence a host of other demographic
663 processes, such as mortality rate, time to maturity, and fecundity, that cumulatively impact

individual fitness and species population dynamics (Madsen and Shine 2000; Dmitriew 2011). Therefore, any alteration to an individual's growth trajectory has the potential to have cascading effects on population demography. The growth rate declines we observed are well within the natural variation for this species (reviewed in Avens et al. 2017) but their severity varied by life stage. For example, oceanic stage turtle growth rates declined by ~8 % after 2012 but GoM and Atlantic small neritic juvenile growth rates declined by ~20% and ~30%, respectively. Avens et al. (*in review*) determined that the U.S. GoM vs. Atlantic Coast differences in somatic growth may delay Atlantic Kemp's ridley maturity by 2 to 3 years relative to GoM counterparts. Herein, post-2012 GoM Kemp's ridley growth rates are similar to those of pre-2012 Atlantic Kemp's ridleys, which suggests a multi-year delay in maturation for GoM turtles is possible. Moreover, the proportionally greater decline in Atlantic Kemp's ridley growth rates may further deepen their life-long disadvantage relative to GoM conspecifics. Integration of somatic growth data into demographic models may shed important light on the impacts of these growth changes on sea turtle population dynamics and implications for conservation and management.

Conclusion

Through analyses of 30 years of dead stranded turtle humeri, we examined the somatic growth response of the critically endangered Kemp's ridley sea turtle to multiple environmental factors. We identified a simultaneous decrease in growth rates beginning in 2012 for oceanic and small neritic juveniles that stranded in U.S. waters. We hypothesize that these changes are due in part to deleterious effects of the *DWH* oil spill on sea turtles and their GoM habitats. For certain life stages, this growth response may reflect synergistic effects of the *DWH* oil spill, climate variability, and density-dependent processes. Our understanding of the links between the *DWH*

687 oil spill and sea turtle growth rates may be greatly enhanced through geochemical analyses (e.g.
688 PAHs, trace elements, isotopes) of turtle bone tissues, which may reveal direct evidence of
689 exposure to *DWH*-associated environmental toxins (e.g., Wise et al. 2014; Wilson et al. 2015;
690 López-Duarte et al. 2016; Romero et al. 2018). This study highlights the critical importance of
691 long-term, continuous collection of sea turtle humerus bones for status and threat assessment. To
692 date, the collection of dead stranded turtle humeri has been inconsistent across both space and
693 time and we lack any knowledge of growth rates of Kemp's ridleys within Mexican waters,
694 where approximately 18% of adult females and an unknown proportion of juveniles forage.
695 Within the U.S., widespread collection of Kemp's ridley bones ended in 2015 but resumption of
696 these efforts and initiation of bone collection in Mexico will be necessary to fully evaluate the
697 long-term influence of these environmental factors on sea turtle growth rates.
698
699 **Compliance with ethical standards**
700 *Conflict of interest*. The authors declare they have no conflict of interest.
701 *Ethical approval*. This article does not contain any studies with human participants or live
702 animals performed by any of the authors.
703
704 **Data availability**
705 The dataset generated and analyzed in the current study are available from the corresponding
706 author upon reasonable request.
707
708 **Acknowledgements**

We thank the hundreds of federal, state, and private partners that collectively form the Sea Turtle Stranding and Salvage Network for their invaluable work without which this study would not have been possible. We also thank K. Magnusson for providing lab space and equipment for skeletochronological analysis, the Oregon State University Linus Pauling Institute for use of their imaging systems, and B. Stacy and J. Keene (NOAA) for collection of humeri associated with the DWH Natural Resource Damage Assessment. Thank you to J. Cordeiro, M. Davis, H. Hagler, and M. VanBemmel for assistance with laboratory analyses. Thank you also to J. Miller, A. Shiel, J. McKay, and two anonymous reviewers for comments on this manuscript. Funding for M. Ramirez and this project were provided by the NSF Graduate Research Fellowship Program. The contents of this publication are solely the responsibility of the authors and do not necessarily represent the official views of the U.S. Department of Commerce, National Oceanic and Atmospheric Administration. Research was conducted under USFWS permit number TE-676379-5 issued to the NMFS Southeast Fisheries Science Center.

References

Albers PH (2006) Birds and polycyclic aromatic hydrocarbons. Avian Poult Biol Rev 17:125–140. doi: 10.3184/147020606783438740

Avens L, Snover ML (2013) Age and age estimation in sea turtles. In: Wyneken J, Lohmann KJ, Musick JA (eds) The Biology of Sea Turtles. CRC Press, Boca Raton, FL, pp 97–134

Avens L, Goshe LR, Coggins L, Shaver DJ, Higgins B, Landry AM, Bailey R (2017) Variability in age and size at maturation, reproductive longevity, and long-term growth dynamics for Kemp's ridley sea turtles in the Gulf of Mexico. PLoS ONE 12:e0173999. doi: 10.1371/journal.pone.0173999

Avens L, Ramirez MD, Hall AG, Snover ML, Haas HL, Godfrey MH, Goshe LR, Cook M, Heppell SS (in review) Regional differences in Kemp's ridley sea turtle growth trajectories and expected age at maturation. Mar Ecol Prog Ser

Baty F, Ritz C, Charles S, Brutsche M, Flandrois J-P, Delignette-Muller M-L (2015) A toolbox for nonlinear regression in *R*: the package nlstools. J Stat Softw. doi: 10.18637/jss.v066.i05

Beaugrand G, McQuatters-Gollop A, Edwards M, Goberville E (2013) Long-term responses of North Atlantic calcifying plankton to climate change. Nat Clim Change 3:263–267. doi: 10.1038/nclimate1753

Berenshtein I, Paris CB, Perlin N, Alloy MM, Joye SB, Murawski S (2020) Invisible oil beyond the *Deepwater Horizon* satellite footprint. Sci Adv 6:eaaw8863. doi: 10.1126/sciadv.aaw8863

Bevan E, Wibbels T, Najera BMZ, Sarti L, Martinez FI, Cuevas JM, Gallaway BJ, Pena LJ, Burchfield PM (2016) Estimating the historic size and current status of the Kemp's ridley sea turtle (*Lepidochelys kempii*) population. Ecosphere 7:e01244. doi: 10.1002/ecs2.1244

Beyer J, Trannum HC, Bakke T, Hodson PV, Collier TK (2016) Environmental effects of the Deepwater Horizon oil spill: A review. Mar Pollut Bull 110:28–51. doi: 10.1016/j.marpolbul.2016.06.027

Bjorndal KA, Schroeder BA, Foley AM, Witherington BE, Bresette M, Clark D, Herren RM, Arendt MD, Schmid JR, Meylan AB, Meylan PA, Provancha JA, Hart KM, Lamont MM, Carthy RR, Bolten AB (2013) Temporal, spatial, and body size effects on growth rates of loggerhead sea turtles (*Caretta caretta*) in the Northwest Atlantic. Mar Biol 160:2711–2721. doi: 10.1007/s00227-013-2264-y

Bjorndal KA, Chaloupka M, Saba VS, Diez CE, van Dam RP, Krueger BH, Horrocks JA, Santos AJB, Bellini C, Marcovaldi MAG, Nava M, Willis S, Godley BJ, Gore S, Hawkes LA, McGowan A, Witt MJ, Stringell TB, Sanghera A, Richardson PB, Broderick AC, Phillips Q, Calosso MC, Claydon JAB, Blumenthal J, Moncada F, Nodarse G, Medina Y, Dunbar SG, Wood LD, Lagueux CJ, Campbell CL, Meylan AB, Meylan PA, Burns Perez VR,

760 Coleman RA, Strindberg S, Guzmán-H. V, Hart KM, Cherkiss MS, Hillis-Starr Z,
761 Lundgren IF, Boulon RH, Connett S, Outerbridge ME, Bolten AB (2016) Somatic growth
762 dynamics of West Atlantic hawksbill sea turtles: a spatio-temporal perspective.
763 Ecosphere 7:e01279. doi: 10.1002/ecs2.1279

764 Bjorndal KA, Bolten AB, Chaloupka M, Saba VS, Bellini C, Marcovaldi MAG, Santos AJB,
765 Bortolon LFW, Meylan AB, Meylan PA, Gray J, Hardy R, Brost B, Bresette M, Gorham
766 JC, Connett S, Crouchley BVS, Dawson M, Hayes D, Diez CE, van Dam RP, Willis S,
767 Nava M, Hart KM, Cherkiss MS, Crowder AG, Pollock C, Hillis-Starr Z, Muñoz Tenería
768 FA, Herrera-Pavón R, Labrada-Martagón V, Lorences A, Negrete-Philippe A, Lamont
769 MM, Foley AM, Bailey R, Carthy RR, Scarpino R, McMichael E, Provancha JA, Brooks
770 A, Jardim A, López-Mendilaharsu M, González-Paredes D, Estrades A, Fallabrino A,
771 Martínez-Souza G, Vélez-Rubio GM, Boulon RH, Collazo JA, Wershoven R, Hernández
772 VG, Stringell TB, Sanghera A, Richardson PB, Broderick AC, Phillips Q, Calosso M,
773 Claydon JAB, Metz TL, Gordon AL, Landry AM, Shaver DJ, Blumenthal J, Collyer L,
774 Godley BJ, McGowan A, Witt MJ, Campbell CL, Lagueux CJ, Bethel TL, Kenyon L
775 (2017) Ecological regime shift drives declining growth rates of sea turtles throughout the
776 West Atlantic. Glob Change Biol 4556–4568. doi: 10.1111/gcb.13712

777 Brown-Peterson NJ, Krasnec MO, Lay CR, Morris JM, Griffitt RJ (2016) Responses of juvenile
778 southern flounder exposed to Deepwater Horizon oil-contaminated sediments. Environ
779 Toxicol Chem 1–10. doi: 10.1002/etc.3629

780 Burnham KP, Anderson DR (2002) Model selection and multimodel inference: a practical
781 information-theoretic approach, 2nd ed. Springer, New York

782 Byles RA (1988) Behavior and ecology of sea turtles from Chesapeake Bay, Virginia. Doctoral
783 Dissertation, The College of William & Mary

784 Caillouet CW (2014) Interruption of the Kemp's ridley population's pre-2010 exponential
785 growth in the Gulf of Mexico and its aftermath: one hypothesis. Mar Turt Newsl 143:1–7.

786 Caillouet CW (2019) Excessive annual numbers of neritic immature kemp's ridleys may prevent
787 population recovery. Mar Turt Newsl 158:1–9.

788 Caillouet CW, Shaver DJ, Landry Jr AM (2015) Kemp's ridley sea turtle (*Lepidochelys kempii*)
789 head-start and reintroduction to Padre Island National Seashore, Texas. Herpetol Conserv
790 Biol 10:309–377.

791 Caillouet CW, Gallaway BJ, Putman NF (2016) Kemp's ridley sea turtle saga and setback: novel
792 analyses of cumulative hatchlings released and time-lagged annual nests in Tamaulipas,
793 Mexico. Chelonian Conserv Biol 15:115–131. doi: 10.2744/CCB-1189.1

794 Caillouet CW, Raborn SW, Shaver DJ, Putman NF, Gallaway BJ, Mansfield KL (2018) Did
795 declining carrying capacity for the Kemp's Ridley sea turtle population within the Gulf of
796 Mexico contribute to the nesting setback in 2010−2017? Chelonian Conserv Biol 17:123–
797 133. doi: 10.2744/CCB-1283.1

798 Coleman AT, Pulis EE, Pitchford JL, Crocker K, Heaton AJ, Carron AM, Hatchett W, Shannon
799 D, Austin F, Dalton M, others (2016) Population ecology and rehabilitation of
800 incidentally captured Kemp's ridley sea turtles (*Lepidochelys kempii*) in the Mississippi
801 Sound, USA. Herpetol Conserv Biol 11:253–264.

802 Crain CM, Kroeker K, Halpern BS (2008) Interactive and cumulative effects of multiple human
803 stressors in marine systems. Ecol Lett 11:1304–1315. doi: 10.1111/j.1461-
804 0248.2008.01253.x

805 Dmitriew CM (2011) The evolution of growth trajectories: what limits growth rate? Biol Rev
806 86:97–116. doi: 10.1111/j.1469-185X.2010.00136.x

807 Dormann CF, Elith J, Bacher S, Buchmann C, Carl G, Carré G, Marquéz JRG, Gruber B,
808 Lafourcade B, Leitão PJ, Münkemüller T, McClean C, Osborne PE, Reineking B,
809 Schröder B, Skidmore AK, Zurell D, Lautenbach S (2013) Collinearity: a review of
810 methods to deal with it and a simulation study evaluating their performance. Ecography
811 36:27–46. doi: 10.1111/j.1600-0587.2012.07348.x

812 Drinkwater KF, Belgrano A, Borja A, Conversi A, Edwards M, Greene CH, Ottersen G,
813 Pershing AJ, Walker H (2003) The response of marine ecosystems to climate variability
814 associated with the North Atlantic Oscillation. In: Hurrell JW, Kushnir Y, Ottersen G,
815 Visbeck M (eds) Geophysical Monograph Series. American Geophysical Union,
816 Washington, D. C., pp 211–234

817 DWH NRDA Trustees (2016) Deepwater Horizon Oil Spill: Final Programmatic Damage
818 Assessment and Restoration Plan and Final Programmatic Environmental Impact
819 Statement. Department of Commerce and National Oceanic and Atmospheric
820 Administration

821 Edwards M, Beaugrand G, Helaouët P, Alheit J, Coombs S (2013) Marine ecosystem response to
822 the Atlantic Multidecadal Oscillation. PLoS ONE 8:e57212. doi:
823 10.1371/journal.pone.0057212

824 Francis R (1990) Back-calculation of fish length: a critical review. J Fish Biol 36:883–902.

825 Gaillard J-M, Loison A, ToÏgo C, Delorme D, Laere GV (2003) Cohort effects and deer
826 population dynamics. Écoscience 10:412–420. doi: 10.1080/11956860.2003.11682789

827 Gallaway BJ, Gazey WJ, Wibbels T, Bevan E, Shaver DJ, George J (2016) Evaluation of the
828 status of the Kemp's ridley sea turtle after the 2010 Deepwater Horizon oil spill. Gulf
829 Mex Sci 33:192–205.

830 Giannini A, Chiang JCH, Cane MA, Kushnir Y, Seager R (2001) The ENSO Teleconnection to
831 the tropical Atlantic Ocean: contributions of the remote and local SSTs to rainfall
832 variability in the topical Americas. J Clim 14:4530–4544. doi: 10.1175/1520-
833 0442(2001)014<4530:TETTTT>2.0.CO;2

834 Gower J, Young E, King S (2013) Satellite images suggest a new Sargassum source region in
835 2011. Remote Sens Lett 4:764–773. doi: 10.1080/2150704X.2013.796433

836 Greene CH, Meyer-Gutbrod E, Monger BC, McGarry LP, Pershing AJ, Belkin IM, Fratantoni
837 PS, Mountain DG, Pickart RS, Proshutinsky A, Ji R, Bisagni JJ, Hakkinen SMA,
838 Haidvogel DB, Wang J, Head E, Smith P, Reid PC, Conversi A (2013) Remote climate
839 forcing of decadal-scale regime shifts in Northwest Atlantic shelf ecosystems. Limnol
840 Oceanogr 58:803–816. doi: 10.4319/lo.2013.58.3.0803

841 GSMFC (2015) The blue crab fishery of the Gulf of Mexico: a regional management plan. Gulf
842 State Marine Fisheries Commission, Ocean Springs, MS

843 Halpern BS, Walbridge S, Selkoe KA, Kappel CV, Micheli F, D'Agrosa C, Bruno JF, Casey KS,
844 Ebert C, Fox HE, Fujita R, Heinemann D, Lenihan HS, Madin EMP, Perry MT, Selig
845 ER, Spalding M, Steneck R, Watson R (2008) A global map of human impact on marine
846 ecosystems. Science 319:948–952. doi: 10.1126/science.1149345

847 Hart KM, Lamont MM, Sartain AR, Fujisaki I (2014) Migration, foraging, and residency
848 patterns for northern Gulf loggerheads: implications of local threats and international
849 movements. PLoS ONE 9:e103453. doi: 10.1371/journal.pone.0103453

850 Henderson ME, Mills KE, Thomas AC, Pershing AJ, Nye JA (2017) Effects of spring onset and
851 summer duration on fish species distribution and biomass along the Northeast United
852 States continental shelf. Rev Fish Biol Fish 27:411–424. doi: 10.1007/s11160-017-9487-
853 9

854 Heppell SS, Caswell H, Crowder LB (2000) Life histories and elasticity patterns: perturbation
855 analysis for species with minimal demographic data. Ecology 81:654. doi:
856 10.2307/177367

857 Heppell SS, Crouse DT, Crowder LB, Epperly SP, Gabriel W, Henwood T, Marquez R,
858 Thompson NB (2004) A population model to estimate recovery time, population size and
859 management impacts on Kemp's ridley sea turtles. Chelonian Conserv Biol 4:765–771.

860 Heppell SS, Burchfield PM, Pena LJ (2007) Kemp's ridley recovery: how far have we come, and
861 where are we headed? In: Plotkin PT (ed) Biology and Conservation of Ridley Sea
862 Turtles. Johns Hopkins University Press, Baltimore, M.D., pp 325–335

863 Herdter ES, Chambers DP, Stallings CD, Murawski SA (2017) Did the *Deepwater Horizon* oil
864 spill affect growth of Red Snapper in the Gulf of Mexico? Fish Res 191:60–68. doi:
865 10.1016/j.fishres.2017.03.005

866 Hothorn T, Lausen B (2003) On the exact distribution of maximally selected rank statistics.
867 Comput Stat Data Anal 43:121–137. doi: 10.1016/S0167-9473(02)00225-6

868 Hothorn T, Hornik K, van de Wiel MA, Zeileis A (2006) coin: conditional inference procedures
869 in a permutation test framework.

870 Karnauskas M, Schirripa MJ, Craig JK, Cook GS, Kelble CR, Agar JJ, Black BA, Enfield DB,
871 Lindo-Atichati D, Muhling BA, Purcell KM, Richards PM, Wang C (2015) Evidence of
872 climate-driven ecosystem reorganization in the Gulf of Mexico. Glob Change Biol
873 21:2554–2568. doi: 10.1111/gcb.12894

874 Kellar NM, Speakman TR, Smith CR, Lane SM, Balmer BC, Trego ML, Catelani KN, Robbins
875 MN, Allen CD, Wells RS, Zolman ES, Rowles TK, Schwacke LH (2017) Low
876 reproductive success rates of common bottlenose dolphins *Tursiops truncatus* in the
877 northern Gulf of Mexico following the Deepwater Horizon disaster (2010-2015).
878 Endanger Species Res 33:143–158. doi: 10.3354/esr00775

879 Kocmoud AR, Wang H-H, Grant WE, Gallaway BJ (2019) Population dynamics of the
880 endangered Kemp's ridley sea turtle following the 2010 oil spill in the Gulf of Mexico:
881 Simulation of potential cause-effect relationships. Ecol Model 392:159–178. doi:
882 10.1016/j.ecolmodel.2018.11.014

883 Lamont MM, Fujisaki I (2014) Effects of ocean temperature on nesting phenology and fecundity
884 of the loggerhead sea turtle (*Caretta caretta*). J Herpetol 48:98–102. doi: 10.1670/12-
885 217

886 Lane SM, Smith CR, Mitchell J, Balmer BC, Barry KP, McDonald T, Mori CS, Rosel PE,
887 Rowles TK, Speakman TR, Townsend FI, Tumlin MC, Wells RS, Zolman ES, Schwacke
888 LH (2015) Reproductive outcome and survival of common bottlenose dolphins sampled
889 in Barataria Bay, Louisiana, USA, following the *Deepwater Horizon* oil spill. Proc R Soc
890 B 282:20151944. doi: 10.1098/rspb.2015.1944

891 Larsson K, Forslund P (1991) Environmentally induced morphological variation in the Barnacle
892 Goose, Branta leucopsis. J Evol Biol 4:619–636. doi: 10.1046/j.1420-
893 9101.1991.4040619.x

894 López-Duarte PC, Fodrie FJ, Jensen OP, Whitehead A, Galvez F, Dubansky B, Able KW (2016)
895 Is exposure to Macondo oil reflected in the otolith chemistry of marsh-resident fish?
896 PLoS ONE 11:e0162699. doi: 10.1371/journal.pone.0162699

897 Luczak C., Beaugrand G., Jaffré M., Lenoir S. (2011) Climate change impact on Balearic
898 shearwater through a trophic cascade. Biol Lett 7:702–705. doi: 10.1098/rsbl.2011.0225

899 Madsen T, Shine R (2000) Silver spoons and snake body sizes: prey availability early in life
900 influences long-term growth rates of free-ranging pythons. J Anim Ecol 69:952–958. doi:
901 10.1111/j.1365-2656.2000.00477.x

902 McAdam AG, Boutin S (2003) Effects of food abundance on genetic and maternal variation in
903 the growth rate of juvenile red squirrels. J Evol Biol 16:1249–1256. doi: 10.1046/j.1420-
904 9101.2003.00630.x

905 McCauley DJ, Pinsky ML, Palumbi SR, Estes JA, Joyce FH, Warner RR (2015) Marine
906 defaunation: Animal loss in the global ocean. Science 347:1255641–1255641. doi:
907 10.1126/science.1255641

McDonald T, Schroeder B, Stacy B, Wallace B, Starcevich L, Gorham J, Tumlin M, Cacela D, Rissing M, McLamb D, Ruder E, Witherington B (2017) Density and exposure of surface-pelagic juvenile sea turtles to *Deepwater Horizon* oil. Endanger Species Res 33:69–82. doi: 10.3354/esr00771

Meador JP, Sommers FC, Ylitalo GM, Sloan CA (2006) Altered growth and related physiological responses in juvenile Chinook salmon (*Oncorhynchus tshawytscha*) from dietary exposure to polycyclic aromatic hydrocarbons (PAHs). Can J Fish Aquat Sci 63:2364–2376. doi: 10.1139/f06-127

Mills K, Pershing A, Brown C, Chen Y, Chiang F-S, Holland D, Lehuta S, Nye J, Sun J, Thomas A, Wahle R (2013) Fisheries management in a changing climate: Lessons from the 2012 ocean heat wave in the Northwest Atlantic. Oceanography. doi: 10.5670/oceanog.2013.27

Mitchelmore C, Bishop C, Collier T (2017) Toxicological estimation of mortality of oceanic sea turtles oiled during the *Deepwater Horizon* oil spill. Endanger Species Res 33:39–50. doi: 10.3354/esr00758

Müller J, Hothorn T (2004) Maximally selected two-sample statistics as a new tool for the identification and assessment of habitat factors with an application to breeding-bird communities in oak forests. Eur J For Res 123:219–228. doi: 10.1007/s10342-004-0035-5

Murawski S, Fleeger J, Patterson III W, Hu C, Daly K, Romero I, Toro-Farmer G (2016) How did the Deepwater Horizon oil spill affect coastal and continental shelf ecosystems of the Gulf of Mexico? Oceanography 29:160–173. doi: 10.5670/oceanog.2016.80

Musick JA, Limpus CJ (1997) Habitat utilization and migration in juvenile sea turtles. In: Lutz PL, Musick JA (eds) The Biology of Sea Turtles. CRC Press, Boca Raton, FL, pp 137–164

NMFS, USFWS (2015) Kemp's ridley sea turtle (*Lepidochelys kempii*) 5-year review: summary and evaluation. National Marine Fisheries Service, Silver Spring, MD

Ogle DH, Wheeler P, Dinno A (2018) FSA: fisheries stock analysis.

Parham JF, Zug GR (1997) Age and growth of loggerhead sea turtles (*Caretta caretta*) of coastal Georgia: an assessment of skeletochronological age-estimates. Bull Mar Sci 61:287–304.

Perez CR, Moye JK, Cacela D, Dean KM, Pritsos CA (2017) Body mass change in flying homing pigeons externally exposed to *Deepwater Horizon* crude oil. Ecotoxicol Environ Saf 146:104–110. doi: 10.1016/j.ecoenv.2017.05.012

Pershing A, Mills K, Dayton A, Franklin B, Kennedy B (2018) Evidence for adaptation from the 2016 Marine heatwave in the Northwest Atlantic Ocean. Oceanography. doi: 10.5670/oceanog.2018.213

943 Pershing AJ, Alexander MA, Hernandez CM, Kerr LA, Le Bris A, Mills KE, Nye JA, Record
944 NR, Scannell HA, Scott JD, Sherwood GD, Thomas AC (2015) Slow adaptation in the
945 face of rapid warming leads to collapse of the Gulf of Maine cod fishery. Science
946 350:809–812. doi: 10.1126/science.aac9819

947 Peterson CH, Rice SD, Short JW, Esler D, Bodkin JL, Ballachey BE, Irons DB (2003) Long-
948 term ecosystem response to the Exxon Valdez oil spill. Science 302:2082–2086.

949 Powers SP, Hernandez FJ, Condon RH, Drymon JM, Free CM (2013) Novel pathways for injury
950 from offshore oil spills: direct, sublethal and indirect effects of the *Deepwater Horizon*
951 oil spill on pelagic *Sargassum* communities. PLoS ONE 8:e74802. doi:
952 10.1371/journal.pone.0074802

953 Putman NF, Mansfield KL, He R, Shaver DJ, Verley P (2013) Predicting the distribution of
954 oceanic-stage Kemp's ridley sea turtles. Biol Lett 9:20130345. doi:
955 10.1098/rsbl.2013.0345

956 Putman NF, Abreu-Grobois FA, Iturbe-Darkistade I, Putman EM, Richards PM, Verley P (2015)
957 Deepwater Horizon oil spill impacts on sea turtles could span the Atlantic. Biol Lett
958 11:20150596. doi: 10.1098/rsbl.2015.0596

959 R Core Team (2019) R: A language and environment for statistical computing.

960 Reich KJ, López-Castro MC, Shaver DJ, Iseton C, Hart KM, Hooper MJ, Schmitt CJ (2017) $\delta^{13}C$
961 and $\delta^{15}N$ in the endangered Kemp's ridley sea turtle *Lepidochelys kempii* after the
962 *Deepwater Horizon* oil spill. Endanger Species Res 33:281–289. doi: 10.3354/esr00819

963 Reid PC, Beaugrand G (2012) Global synchrony of an accelerating rise in sea surface
964 temperature. J Mar Biol Assoc UK 92:1435–1450. doi: 10.1017/S0025315412000549

965 Ramirez MD, Avens L, Goshe LR, Snover ML, Cook M and Heppell SS (2020) Regional
966 variation in Kemp's ridley sea turtle diet composition and its potential relationship with
967 somatic growth. Front Mar Sci 7:253. doi: 10.3389/fmars.2020.00253

968 Rocha J, Yletyinen J, Biggs R, Blenckner T, Peterson G (2014) Marine regime shifts: drivers and
969 impacts on ecosystems services. Phil Trans R Soc B 370:20130273 doi:
970 10.1098/rstb.2013.0273

971 Romero IC, Toro-Farmer G, Diercks A-R, Schwing P, Muller-Karger F, Murawski S, Hollander
972 DJ (2017) Large-scale deposition of weathered oil in the Gulf of Mexico following a
973 deep-water oil spill. Environ Pollut 228:179–189. doi: 10.1016/j.envpol.2017.05.019

974 Romero IC, Sutton T, Carr B, Quintana-Rizzo E, Ross SW, Hollander DJ, Torres JJ (2018)
975 Decadal assessment of polycyclic aromatic hydrocarbons in mesopelagic fishes from the
976 Gulf of Mexico reveals exposure to oil-derived sources. Environ Sci Technol 52:10985–
977 10996. doi: 10.1021/acs.est.8b02243

978 Rouhani S, Baker MC, Steinhoff M, Zhang M, Oehrig J, Zelo IJ, Emsbo-Mattingly SD, Nixon Z,
979 Willis JM, Hester MW (2017) Nearshore exposure to *Deepwater Horizon* oil. Mar Ecol
980 Prog Ser 576:111–124. doi: 10.3354/meps11811

981 Rozas LP, Minello TJ, Miles MS (2014) Effect of Deepwater Horizon oil on growth rates of
982 juvenile Penaeid shrimps. Estuaries Coasts 37:1403–1414. doi: 10.1007/s12237-013-
983 9766-1

984 Rudloe A, Rudloe J (2005) Site specificity and the impact of recreational fishing activity on
985 subadult endangered Kemp's ridley sea turtles in estuarine foraging habitats in the
986 northeastern Gulf of Mexico. Gulf Mex Sci. doi: 10.18785/goms.2302.05

987 Sanchez-Rubio G, Perry HM, Biesiot PM, Johnson DR, Lipcius RN (2011) Climate-related
988 hydrological regimes and their effects on abundance of juvenile blue crabs (*Callinectes*
989 *sapidus*) in the northcentral Gulf of Mexico. Fish Bull 109:139–146.

990 Sanchez-Rubio G, Perry H, Franks JS, Johnson DR (2018) Occurrence of pelagic *Sargassum* in
991 waters of the U.S. Gulf of Mexico in response to weather-related hydrographic regimes
992 associated with decadal and interannual variability in global climate. Fish Bull 116:93–
993 106.

994 Schmid JR (1998) Marine turtle populations on the West-central coast of Florida: Results of
995 tagging studies at the Cedar Keys, Florida, 1986-1995. Fish Bull 96:589–602.

996 Schwacke L, Thomas L, Wells R, McFee W, Hohn A, Mullin K, Zolman E, Quigley B, Rowles
997 T, Schwacke J (2017) Quantifying injury to common bottlenose dolphins from the
998 *Deepwater Horizon* oil spill using an age-, sex- and class-structured population model.
999 Endanger Species Res 33:265–279. doi: 10.3354/esr00777

1000 Schwacke LH, Smith CR, Townsend FI, Wells RS, Hart LB, Balmer BC, Collier TK, De Guise
1001 S, Fry MM, Guillette LJ, Lamb SV, Lane SM, McFee WE, Place NJ, Tumlin MC, Ylitalo
1002 GM, Zolman ES, Rowles TK (2014) Health of Common Bottlenose Dolphins (*Tursiops*
1003 *truncatus*) in Barataria Bay, Louisiana, following the *Deepwater Horizon* oil spill.
1004 Environ Sci Technol 48:93–103. doi: 10.1021/es403610f

1005 Shaver DJ, Hart KM, Fujisaki I, Rubio C, Sartain AR, Peña J, Burchfield PM, Gamez DG, Ortiz
1006 J (2013) Foraging area fidelity for Kemp's ridleys in the Gulf of Mexico. Ecol Evol
1007 3:2002–2012. doi: 10.1002/ece3.594

1008 Shaver DJ, Rubio C, Shelby Walker J, George J, Amos AF, Reich K, Jones C, Shearer T (2016)
1009 Kemp's ridley sea turtle (*Lepidochelys kempii*) nesting on the Texas coast: geographic,
1010 temporal, and demographic trends through 2014. Gulf Mex Sci. doi:
1011 10.18785/goms.3302.04

1012 Snover ML, Hohn AA (2004) Validation and interpretation of annual skeletal marks in
1013 loggerhead (*Caretta caretta*) and Kemp's ridley (*Lepidochelys kempii*) sea turtles. Fish
1014 Bull 102:682–692.

1015 Snover ML, Hohn AA, Crowder LB, Heppell SS (2007) Age and growth in Kemp's ridley sea
1016 turtles: evidence from mark-recapture and skeletochronology. In: Plotkin PT (ed) Biology
1017 and Conservation of Ridley Sea Turtles. Johns Hopkins University Press, Baltimore,
1018 M.D., pp 89–106

1019 Stacy BA (2015) Summary of necropsy findings for non-visibly oiled sea turtles documented by
1020 stranding response in Alabama, Louisiana, and Mississippi 2010 through 2014.

1021 Stacy N, Field C, Staggs L, MacLean R, Stacy B, Keene J, Cacela D, Pelton C, Cray C, Kelley
1022 M, Holmes S, Innis C (2017) Clinicopathological findings in sea turtles assessed during
1023 the Deepwater Horizon oil spill response. Endanger Species Res 33:25–37. doi:
1024 10.3354/esr00769

1025 Stubbs JL, Marn N, Vanderklift MA, Fossette S, Mitchell NJ (2020) Simulated growth and
1026 reproduction of green turtle (*Chelonia mydas*) under climate change and marine heatwave
1027 scenarios. Ecol Model 431:109185. doi: 10.1016/j.ecolmodel.2020.109185

1028 Turtle Expert Working Group (2000) Assessment update for the Kemp's ridley and loggerhead
1029 sea turtle populations in the western North Atlantic.

1030 VanderKooy S (2013) Stock assessment report GDAR 01: Gulf of Mexico blue crab. Ocean
1031 Springs, MS

1032 Wallace B, Stacy B, Rissing M, Cacela D, Garrison L, Graettinger G, Holmes J, McDonald T,
1033 McLamb D, Schroeder B (2017) Estimating sea turtle exposures to *Deepwater Horizon*
1034 oil. Endanger Species Res 33:51–67. doi: 10.3354/esr00728

1035 Wilson RM, Cherrier J, Sarkodee-Adoo J, Bosman S, Mickle A, Chanton JP (2015) Tracing the
1036 intrusion of fossil carbon into coastal Louisiana macrofauna using natural 14C and 13C
1037 abundances. Deep Sea Res Part II Top Stud Oceanogr. doi: 10.1016/j.dsr2.2015.05.014

1038 Wise JP, Wise JTF, Wise CF, Wise SS, Gianios C, Xie H, Thompson WD, Perkins C, Falank C,
1039 Wise JP (2014) Concentrations of the genotoxic metals, Chromium and Nickel, in
1040 Whales, tar balls, oil slicks, and released oil from the Gulf of Mexico in the immediate
1041 aftermath of the Deepwater Horizon oil crisis: Is genotoxic metal exposure part of the
1042 Deepwater Horizon legacy? Environ Sci Technol 48:2997–3006. doi: 10.1021/es405079b

1043 Witherington B (2002) Ecology of neonate loggerhead turtles inhabiting lines of downwelling
1044 near a Gulf Stream front. Mar Biol 140:843–853. doi: 10.1007/s00227-001-0737-x

1045 Witherington B, Hirama S, Hardy R (2012) Young sea turtles of the pelagic *Sargassum*-
1046 dominated drift community: habitat use, population density, and threats. Mar Ecol Prog
1047 Ser 463:1–22. doi: 10.3354/meps09970

1048 Witzell WN, Schmid JR (2004) Immature sea turtles in Gullivan Bay, Ten Thousand Islands,
1049 southwest Florida. Gulf Mex Sci. doi: 10.18785/goms.2201.05

1050 Wood SN (2006) Generalized Additive Models: an introduction with R. Chapman and
1051 Hall/CRC, Boca Raton, FL

1052 Ylitalo G, Collier T, Anulacion B, Juaire K, Boyer R, da Silva D, Keene J, Stacy B (2017)
1053 Determining oil and dispersant exposure in sea turtles from the northern Gulf of Mexico
1054 resulting from the *Deepwater Horizon* oil spill. Endanger Species Res 33:9–24. doi:
1055 10.3354/esr00762

1056 Zeileis A, Leisch F, Hornik K, Kleiber C (2002) strucchange: An R Package for Testing for
1057 Structural Change in Linear Regression Models. J Stat Softw 7:1–38.

1058 Zug GR, Wynn AH, Ruckdeschel C (1986) Age determination of loggerhead sea turtles, *Caretta*
1059 *caretta*, by incremental growth marks in the skeleton. Smithson Contrib Zool 427:1–44.

1060

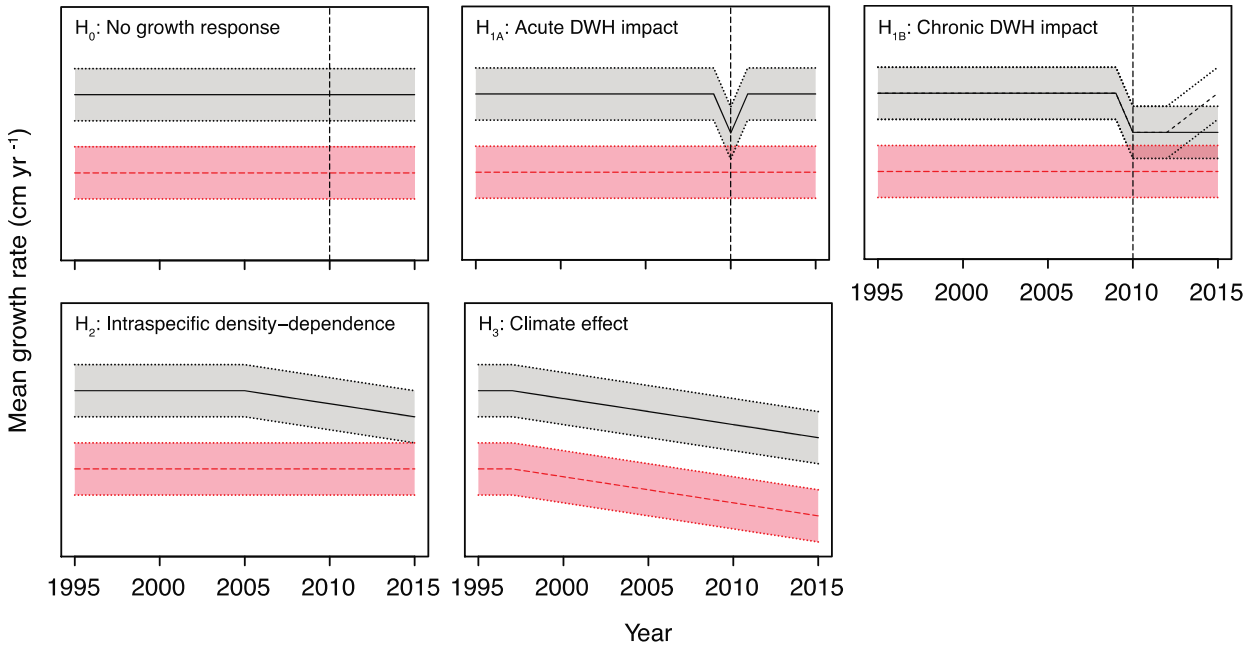

1061

1062 **Fig. 1** Conceptual model of alternative hypotheses for the size class-specific growth response of
1063 Kemp's ridley sea turtles to environmental factors examined herein. All Kemp's ridleys first
1064 reside in oceanic habitats in the central Gulf of Mexico (GoM) for 1–3 years then recruit to
1065 neritic habitats along either the GoM or U.S. Atlantic Coast. The shaded areas represent growth
1066 variation for GoM (black lines, grey shading) and Atlantic (red lines, red shading) life stages.
1067 Vertical dashed lines identify the year of the *Deepwater Horizon* (*DWH*) oil spill (2010). H_0 = no
1068 growth response in turtles from either geographic region or life stage to any factor examined. H_1
1069 = acute or chronic *DWH* oil spill-induced growth response for GoM life stages only (oceanic and
1070 neritic); no growth response in Atlantic neritic life stages due to geographic isolation from *DWH*
1071 oil spill, although Atlantic turtles may exhibit a past response during their GoM oceanic life
1072 stage. H_2 = density-dependent decline in somatic growth beginning in the mid-2000s during
1073 period of exponential population growth; effect in GoM turtles only as > 80 % of the population
1074 is thought to reside in the GoM (Putman et al. 2013; NMFS and USFWS 2015). H_3 = declining
1075 growth beginning in the late 1990s in response to climate-driven ecological regime shift

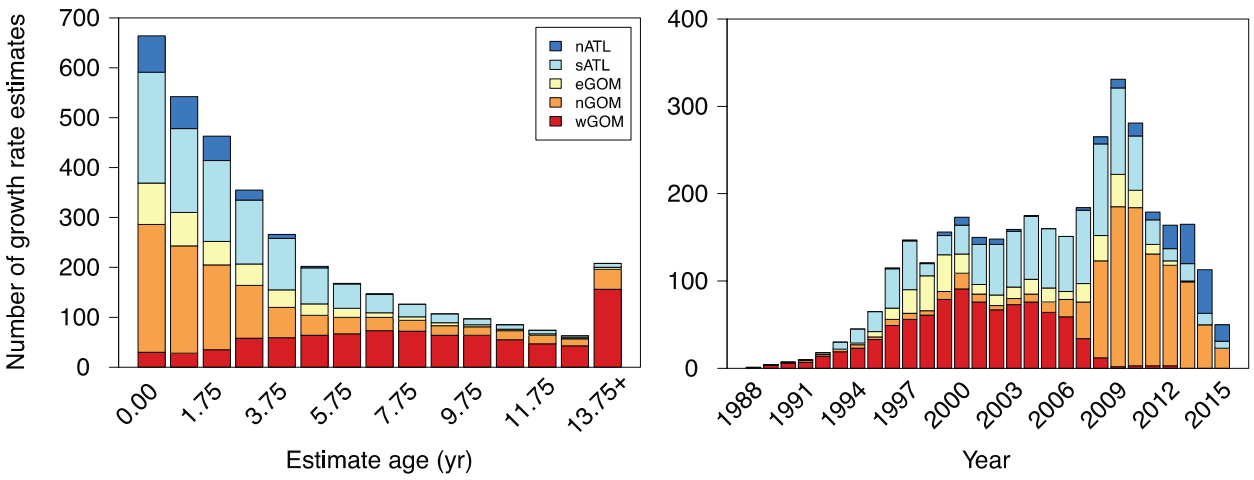

1076

1077 **Fig. 2** Frequency histograms of Kemp's ridley sea turtle back-calculated somatic growth rates by

1078 stranding location, age, and year. nATL = northern Atlantic (stranding location = Delaware, New

1079 Jersey, New York, Massachusetts), sATL = southern Atlantic (stranding location = Atlantic coast

1080 of Florida, Georgia, South Carolina, North Carolina, Virginia), eGoM = eastern Gulf of Mexico

1081 (stranding location = GoM coast of Florida), nGoM = northern Gulf of Mexico (stranding

1082 location = Louisiana, Mississippi, Alabama), wGoM = western Gulf of Mexico (stranding

1083 location = Texas)

1084

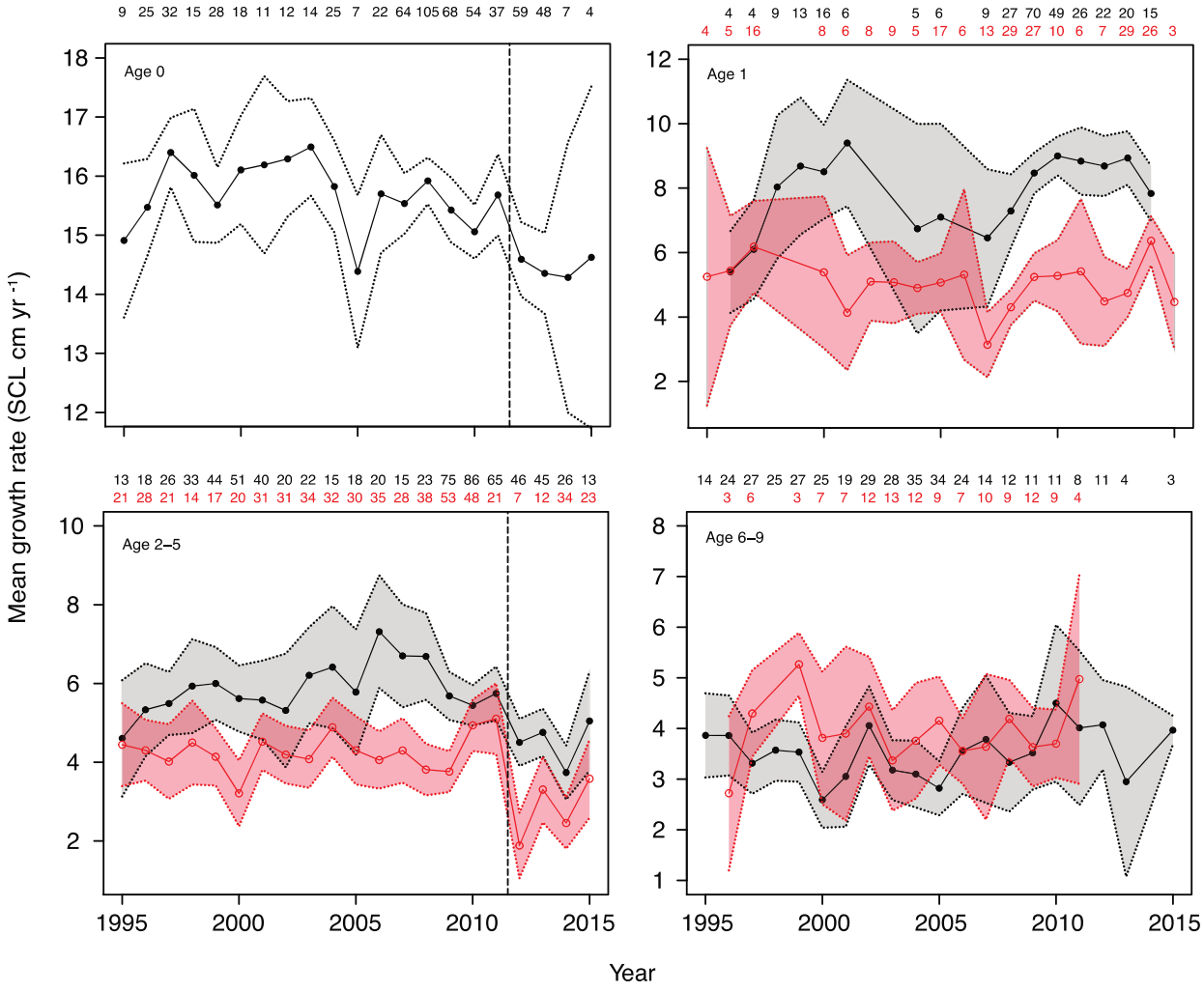

Fig. 3 Time series of mean Kemp's ridley sea turtle growth rate by age class. Dotted lines bound 95% confidence intervals. Age 0 includes data from both Gulf of Mexico (GoM) and Atlantic stranded turtles given that all Kemp's ridleys share oceanic habitats in the central GoM during the oceanic life stage. For all other age classes, GoM and Atlantic data were analyzed separately due to regional differences in growth rates (black shaded area = Gulf of Mexico stranded turtles; red shaded area = Atlantic stranded turtles). Number of growth observations are presented above each plot. Vertical dashed lines identify significant breaks in each time series where there was concordance among statistical methods evaluated (see Table 3). Data for years with $N < 3$ are excluded. SCL = straightline carapace length

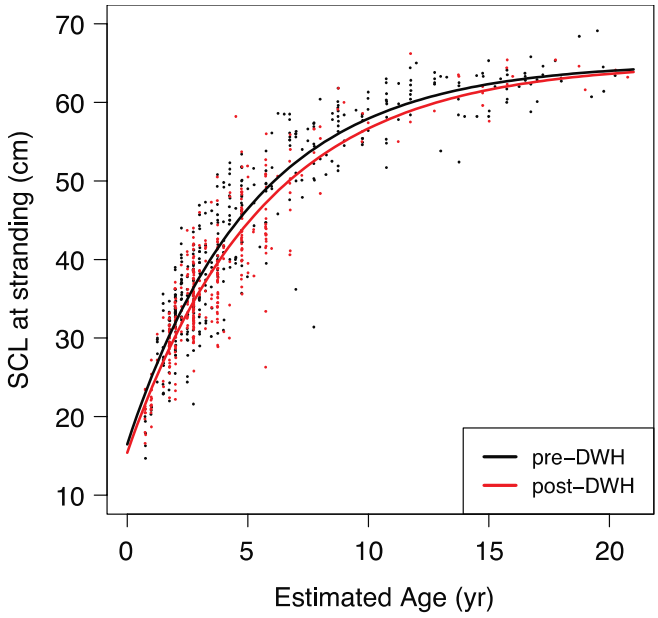

Fig. 4 Von Bertalanffy growth functions estimated for Kemp's ridley sea turtles stranded in the Gulf of Mexico before (1993–2009, $n = 402$) and after (2011–2016, $n = 362$) the *Deepwater Horizon* oil spill. VBGFs were based on measured straightline carapace length (SCL) and estimated age at stranding. Parameter estimates for the best model were $L_\infty = 65.04$, $t_0 = 1.52$, K (pre-*DWH*) = 0.192, and K (post-*DWH*) = 0.178

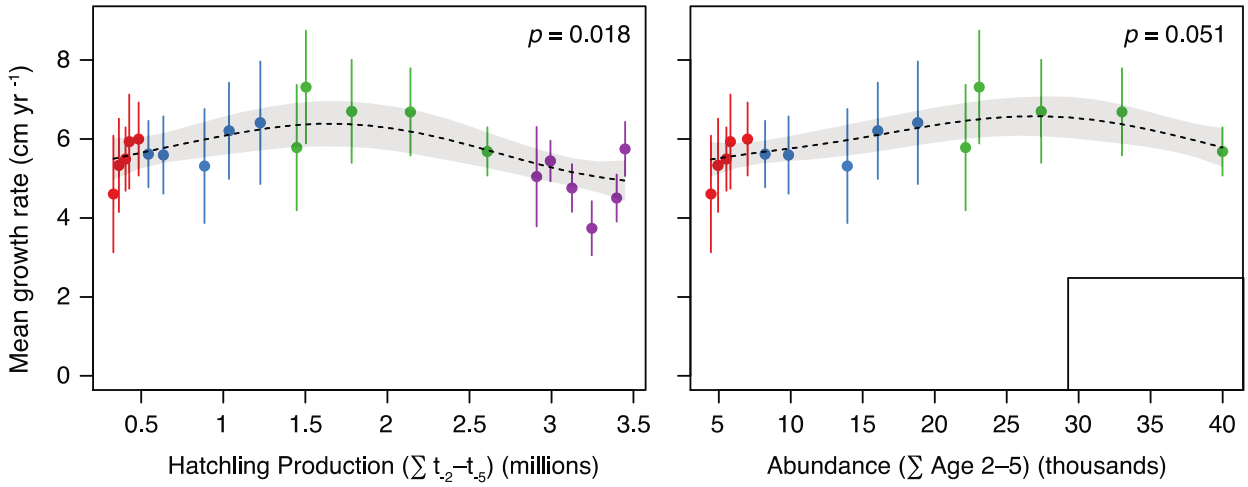

1101

1102 **Fig. 5** Relationship between mean back-calculated growth rate and population density metrics

1103 for age 2–5 Kemp's ridley sea turtles stranded in the Gulf of Mexico. Dashed lines and grey

1104 ribbons are predicted values and 95% CI from GAM models with either cumulative hatchling

1105 production (left panel) or population abundance (right panel) included as a smoother term (see

1106 Table S2). Points are means ± 95% CI. SCL = straightline carapace length. See Figs. S2–S4 for

1107 age 0, age 1, and age 6–9

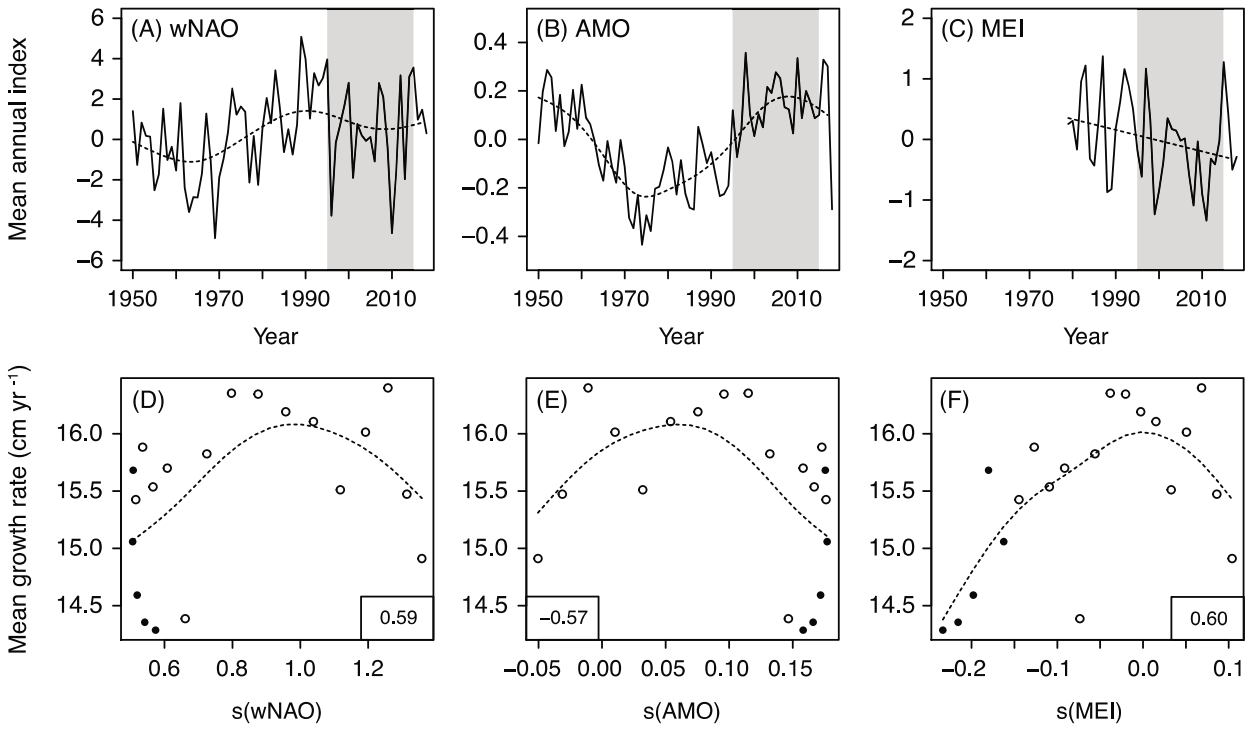

1108

1109 **Fig. 6** Relationships between (**A**-**C**) climate indices and year and (**D**-**F**) mean age 0 growth rates

1110 and annualized climate indices (2-yr lag). Dashed lines are the GAM trends. (**A**-**C**) Shaded area

1111 identifies study period. (**D**-**F**) Cross-correlation values are presented in boxes within each plot.

1112 Open circles are years 1995–2009, whereas filled circles are year 2010–2015. wNAO: Winter

1113 North Atlantic Oscillation, AMO: Atlantic Multidecadal Oscillation, MEI: Multivariate El Niño

1114 Southern Oscillation Index.

Table 1 Summary characteristics for Kemp's ridley sea turtles by stranding location. Western GoM (wGoM) = Texas; northern GoM (nGoM) = Louisiana, Mississippi, Alabama; eastern GoM (eGoM) = GoM coast of Florida); southern Atlantic (sATL) = Atlantic coast of Florida, Georgia, South Carolina, North Carolina, Virginia; northern Atlantic (nATL = Delaware, New Jersey, New York, Massachusetts). See Table S1 for state-specific data

Location	Stranding data				Growth rate data	
	*n**	SCL (cm) Mean ± SD (range)	Estimated age (yr) Mean ± SD (range)	Year range	*n*	Year range
wGoM	200	55.6 ± 10.9 (4.2 – 69.1)	11.87 ± 6.47 (0.00 – 30.25)	1997 – 2013	915	1988 – 2012
nGoM	439	40.0 ± 11.1 (16.6 – 66.2)	4.86 ± 4.37 (0.75 – 23.00)	1993 – 2016	1055	1990 – 2015
eGoM	142	41.1 ± 11.0 (20.3 – 65.4)	4.62 ± 3.23 (1.00 – 15.75)	1998 – 2013	354	1994 – 2013
sATL	362	38.2 ± 10.3 (19.3 – 66.7)	5.07 ± 3.23 (1.00 – 18.75)	1993 – 2016	1071	1990 – 2015
nATL	77	28.0 ± 4.1 (19.3 – 40.0)	3.67 ± 1.41 (1.00 – 8.50)	2001 – 2017	219	1996 – 2015

*Stranding state unknown for 15 turtles (2 in Gulf of Mexico, 13 in Atlantic)

Table 2 Summary statistics for the family of models used to evaluate whether von Bertalanffy growth parameter estimates (L_∞, K, t_0) differed for Kemp's ridley sea turtles stranded in the Gulf of Mexico before (1993–2009, n = 402) and after (2011–2016, n = 362) the *Deepwater Horizon* oil spill. L_∞ is the asymptotic average length, K is the Brody growth rate coefficient, and t_0 is the age when the average length is zero.

Model	*df*	logLik	AIC	ΔAIC	W_i
Common L_∞ and t_0 $(K \neq K)$	5	–2201.34	4412.69	0.00	0.305
Common L_∞ $(K \neq K,\ t_0 \neq t_0)$	6	–2200.37	4412.74	0.05	0.298
Different $L_\infty, K,$ and t_0	7	–2199.91	4413.82	1.13	0.174
Common t_0 $(L_\infty \neq L_\infty,\ K \neq K)$	6	–2201.33	4414.67	1.98	0.113
Common K and t_0 $(L_\infty \neq L_\infty)$	5	–2202.91	4415.81	3.12	0.064
Common K $(L_\infty \neq L_\infty,\ t_0 \neq t_0)$	6	–2202.50	4416.99	4.3	0.036
Common L_∞ and K $(t_0 \neq t_0)$	5	–2204.76	4419.52	6.83	0.010
Common $L_\infty, K,$ and t_0	4	–2214.51	4437.02	24.33	0.000

Table 3 Results of Reverse Helmert regression coding schemes used to compare mean age class-specific growth rates of Kemp's ridley sea turtles before and after the Deepwater Horizon oil spill. Number of asterisks (*) indicates degree of significance based on p-values (* = $p < 0.05$, ** = $p < 0.01$, *** = $p < 0.001$; empty cells mean no significant difference in mean growth rate). Colors indicate direction of change (**black** = increase, **red** = decrease). The complementary cutpoint analyses identified statistically significant structural shift in the age 0, age $2–5_{GoM}$, and age $2–5_{Atlantic}$ growth time series between 2011 and 2012. Years without data for comparison with pre-*DWH* growth rates are noted with a dash

Year comparison	Age class						
	Gulf of Mexico stranded turtles				Atlantic stranded turtles		
Comparison	0	1	2–5	6–9	1	2–5	6–9
2005 vs. 1995–2004				*			
2006 vs. 1995–2005			**				
2007 vs. 1995–2006					**		
2008 vs. 1995–2007							
2009 vs. 1995–2008							
2010 vs. 1995–2009						***	
2011 vs. 1995–2009						**	
2012 vs. 1995–2009	**		*			**	
2013 vs. 1995–2009	***		**				
2014 vs. 1995–2009			***		**	***	*
2015 vs. 1995–2009							–

Table 4 Summary statistics for the family of Generalized Additive Models used to evaluate the influence of covariates [temporal shift (TS), hatchling production (HatchProd), Atlantic Multidecadal Oscillation (AMO)] on mean age class-specific growth rates for age 0 and age 2–5 Kemp's ridley sea turtles. *TS* is a factor with categorization based on breakpoint identified in temporal analyses (pre-shift = 1995–2011, post-shift = 2012–2015). *HatchProd* is cumulative hatchling production for years, t(x), prior to a given year (age 0 = $\Sigma\ t_{0}$–t_{-1}, age 2–5 = $\Sigma\ t_{-2}$–t_{-5}). *AMO* is the annualized GAM trend for the index with a 2-year lag.

Model	*df*	logLik	AIC	ΔAIC	W_i
(a) Age 0					
TS + HatchProd	4.00	–11.28	30.57	0.00	0.32
TS + AMO	5.34	–10.04	30.76	0.19	0.29
TS	3.00	–12.57	31.15	0.58	0.24
TS + AMO + HatchProd	5.00	–11.02	32.05	1.48	0.15
HatchProd	3.00	–20.72	47.45	16.88	0.00
AMO	3.39	–20.69	48.15	17.58	0.00
(b) Age 2–5, Gulf of Mexico					
TS + AMO + HatchProd	5.00	–11.17	32.35	0.00	0.49
TS + HatchProd	6.74	–9.58	32.64	0.29	0.43
TS	3.00	–15.51	37.03	4.68	0.05
TS + AMO	4.00	–14.85	37.71	5.36	0.03
HatchProd	5.46	–16.45	43.83	11.48	0.00
AMO	3.00	–23.51	53.02	20.67	0.00
(c) Age 2–5, Atlantic					
TS	3.00	–14.86	35.72	0.00	0.45
TS + HatchProd	4.00	–14.48	36.95	1.23	0.24
TS + AMO	4.00	–14.83	37.65	1.93	0.17
TS + AMO + HatchProd	5.00	–14.09	38.17	2.45	0.13
HatchProd	3.00	–21.41	48.82	13.10	0.00
AMO	3.00	–21.98	49.97	14.25	0.00

Table 5 Summary of statistical output for Generalized Additive Models (GAMs) used to evaluate the influence of potential environmental covariates [temporal shift (*TS*), hatchling production (*HatchProd*), Atlantic Multidecadal Oscillation (AMO)] on mean age class-specific growth rates for age 0 and age 2–5 Kemp's ridley sea turtles. *TS* is a factor with categorization based on breakpoint identified in temporal analyses (TS_{pre} = 1995–2011, TS_{post} = 2012–2015). *HatchProd* is cumulative hatchling production for years, t(x), prior to a given year (age 0 = $\Sigma\ t_0$–t_{-1}, age 2–5 = $\Sigma\ t_{-2}$–t_{-5}). *AMO* is the annualized GAM trend for the index with a 2-year lag. *Dev* : deviance explained by the model. *Edf*: estimated degrees of freedom. The models are ordered as in Table 4, with age class-specific models with ΔAIC scores < 2 denoted with an asterisk (*). Bold values denote statistically significant covariates ($p < 0.05$)

			Smooth terms				Parametric coefficients				
Model	Dev (%)	Adj. R^2	Var	*Edf*	*F*	Prob(*F*)	Var	Est	SE	t	Pr>|*t*|
(a) Age 0 (*n* = 21 years)											
$GAM_{TS + HatchProd}$*	65.1	0.61	HatchProd	1.00	2.35	0.142	TS_{pre}	1.13	0.22	5.12	**<0.001**
$GAM_{TS + AMO}$*	69.0	0.64	AMO	1.90	2.34	0.235	TS_{pre}	1.13	0.22	5.26	**<0.001**
GAM_{TS}*	60.6	0.59	–	–	–	–	TS_{pre}	1.20	0.22	5.40	**<0.001**
$GAM_{TS + AMO + HatchProd}$*	66.0	0.60	AMO	1.00	0.43	0.522	TS_{pre}	1.15	0.23	5.08	**<0.001**
			HatchProd	1.00	1.30	0.270					
$GAM_{HatchProd}$	14.3	0.10	HatchProd	1.00	3.18	0.091	–	–	–	–	–
GAM_{AMO}	14.6	0.09	AMO	1.21	1.68	0.165	–	–	–	–	–
(b) Age 2–5, Gulf of Mexico (*n* = 21 years)											
$GAM_{TS + AMO + HatchProd}$*	69.2	0.64	AMO	1.00	8.69	**0.009**	TS_{pre}	0.99	0.29	3.38	**0.004**
			HatchProd	1.00	7.14	**0.016**					
$GAM_{TS + HatchProd}$*	73.6	0.67	HatchProd	3.07	2.53	0.072	TS_{pre}	1.07	0.28	3.84	**0.001**
GAM_{TS}	53.5	0.51	–	–	–	–	TS_{pre}	1.29	0.28	4.67	**<0.001**
$GAM_{TS + AMO}$	56.3	0.52	AMO	1.00	1.17	0.294	TS_{pre}	1.39	0.29	4.80	**<0.001**
$GAM_{HatchProd}$	49.1	0.41	HatchProd	2.84	4.11	**0.018**	–	–	–	–	–
GAM_{AMO}	0.4	–0.05	AMO	1.00	0.07	0.793	–	–	–	–	–
(c) Age 2–5, Atlantic (*n* = 21 years)											
GAM_{TS}*	50.0	0.47	–	–	–	–	TS_{pre}	1.39	0.32	4.36	**<0.001**
$GAM_{TS + HatchProd}$*	51.8	0.46	HatchProd	1.00	0.68	0.422	TS_{pre}	1.55	0.38	4.10	**<0.001**
$GAM_{TS + AMO}$*	50.1	0.45	AMO	1.00	0.06	0.808	TS_{pre}	1.40	0.34	4.19	**<0.001**
$GAM_{TS + AMO + HatchProd}$	53.5	0.45	AMO	1.00	0.64	0.433	TS_{pre}	1.69	0.42	4.03	**<0.001**
			HatchProd	1.00	1.24	0.280					
$GAM_{HatchProd}$	6.7	0.02	HatchProd	1.00	1.36	0.257	–	–	–	–	–
GAM_{AMO}	1.4	–0.04	AMO	1.00	0.27	0.604	–	–	–	–	–